CHARLES UNIVERSITY IN PRAGUE
FACULTY OF PHARMACY IN HRADEC KRÁLOVÉ

DEPARTMENT OF PHARMACEUTICAL CHEMISTRY AND DRUG CONTROL

DIPLOMA THESIS

Synthesis of novel blebbistatin derivatives as myosin inhibitors

Supervisors:

Assoc. Prof. RNDr. Veronika Opletalová, Ph.D.

Prof. Dr. Hans-Dieter Arndt

Hradec Králové 2016

Ngoc Lam Pham

ACKNOWLEDGMENT

Firstly, I would like to thank prof. Dr. Hans-Dieter Arndt for giving me the opportunity to join his group and allow me to work on this thesis during my Erasmus+ exchange program. Also I would like to express appreciation to everyone at Institute for Organic Chemistry and Macromolecular Chemistry, Faculty of Chemistry and Earth Science, Friedrich Schiller University Jena for their guidance, support, patience and pleasant working environment.

I would like to express my sincere gratitude to my supervisors Assoc. prof. RNDr. Veronika Opletalová, Ph.D., prof. Dr. Hans-Dieter Arndt and MSc. Eugenie Nepovimová, who lectured me and tirelessly supervised me all the way through.

Last but not least, I would like to thank my family and friends for their support and patience.

Ngoc Lam Pham

DECLARATION

I declare that this thesis is my original copyrighted work. All literature and other resources I used while processing are listed in the bibliography and properly cited. The thesis was not misused for obtaining the same or different academic degree.

Date: 13th May 2016

……..

Ngoc Lam Pham

ABSTRACT

Charles University in Prague

Faculty of Pharmacy in Hradec Králové

Department of Pharmaceutical Chemistry and Drug Control

Student: Ngoc Lam Pham

Supervisor: Assoc. Prof. RNDr. Veronika Opletalová, Ph.D.

Thesis Title: Synthesis of novel blebbistatin derivatives as myosin inhibitors

Myosins constitute a large and diverse superfamily of ATP-dependent motor proteins responsible for actin-based motility. Currently, based on phylogenetic analyses, myosins are classified into at least twenty four groups. The members of this superfamily are involved in several cell processes such as muscle contraction, cytokinesis, organelle transport, cell polarization and signal transduction. Thus, dysfunction and mutation of myosins can cause several diseases.

Therefore, design of myosin inhibitors seems to be very attractive research field from the point of view of characterization of intracellular processes as well as development of novel targeted therapy against diseases implicating myosin dysfunction.

Nowadays, one of the most well-known and widely used inhibitors of myosin is (*S*)-blebbistatin. This inhibitor of myosin II has many advantages, nevertheless it possesses also several limiting factors impeding the biological studies such as photosensitivity and low solubility in water.

The aim of this Thesis was to synthetize novel blebbistatin derivatives in order to improve properties of the inhibitor and eliminate its disadvantageous qualities. Last but not least, novel derivatives were designed to exert higher affinity to particular myosin II isoforms, which could serve to more specific characterization of myosin II functions.

ABSTRAKT

Univerzita Karlova v Praze

Farmaceutická fakulta v Hradci Králové

Katedra farmaceutické chemie a kontroly léčiv

Student: Ngoc Lam Pham

Vedoucí: doc. RNDr. Veronika Opletalová, Ph.D.

Název práce: Syntéza nových derivátů blebbistatinu jako inhibitorů myosinu

Myosiny tvoří velkou a rozmanitou skupinu ATP-dependentních motorových proteinů zodpovědných za motilitu na aktinových vláknech. Současné fylogenetické analýzy rozdělují myosiny do nejméně dvaceti čtyř tříd. Zástupci těchto skupin se podílejí na mnoha buněčných procesech, jako je svalová kontrakce, cytokineze, transport organel, polarizace buňky a transdukce signálu. Proto dysfunkce a mutace myosinu mohou být příčinou některých onemocnění.

Vývoj inhibitorů myosinu se zdá být velice atraktivní oblastí výzkumu z pohledu jak charakterizace vnitřních buněčných procesů, tak i vývoje cílené léčby onemocnění spojených s myosinovou dysfunkcí.

Jedním z nejznámějších a nejpoužívanějších inhibitorů myosinu v současné době je (*S*)-blebbistatin. Využití tohoto inhibitoru jako malého molekulového nástroje má mnoho výhod, přesto se však u něj vyskytují některé limitující faktory, které omezují jeho použití při biologických studiích, jako je například fotosensitivita a nízká rozpustnost ve vodě.

Cílem této práce bylo připravit nové deriváty blebbistatinu za účelem zlepšení biologického profilu tohoto inhibitoru a odstranění jeho nežádoucích vlastností. V neposlední řadě nutno zmínit, že nové deriváty byly navrženy tak, aby vykazovaly vyšší afinitu k jednotlivým izoformám myosinu II, což by napomohlo k podrobnější charakterizaci funkcí myosinu.

CONTENT

1 ABRREVIATIONS 7

2 AIM OF THE WORK 9

3 THEORETICAL PART 10

3.1 MYOSIN SUPERFAMILY 10

3.1.1 INTRODUCTION OF MYOSINS 10

3.1.2 CONVENTIONAL MYOSINS 10

3.1.3 UNCONVENTIONAL MYOSINS 10

3.1.4 MYOSIN STRUCTURE 12

3.1.5 MOLECULAR MECHANISM – ATPASE CYCLE 13

3.1.6 REGULATION OF MYOSIN ACTIVITY 14

3.1.7 DISEASES ASSOCIATED WITH MYOSIN MUTATIONS AND DYSFUNCTIONS 15

3.2 INHIBITORS OF MYOSIN 15

3.3 BLEBBISTATIN 17

3.3.1 INTRODUCTION OF (*S*)-BLEBBISTATIN 17

3.3.2 MECHANISM OF MYOSIN INHIBITION BY BLEBBISTATIN 18

3.3.3 STRUCTURAL BASIS OF MYOSIN INHIBITION BY BLEBBISTATIN 19

3.3.4 PROS AND CONS OF (*S*)-BLEBBISTATIN 21

3.3.5 BLEBBISTATIN DERIVATIVES 22

4 EXPERIMENTAL PART 25

4.1 OPTIMIZATION OF BLEBBISTATIN SYNTHESIS 25

4.2 DESING OF NOVEL BLEBBISTATIN DERIVATIVES 26

4.3 SYNTHESIS OF NOVEL BLEBBISTATIN DERIVATIVES 31

4.3.1 SYNTHESIS OF (*S*)-6-NOR-BLEBBISTATIN (SCHEME 3) 33

4.3.2 SYNTHESIS OF 6-ETHYL ANALOGUE OF BLEBBISTATIN (SCHEME 4) . 36

4.3.3 SYNTHESIS OF 6-BROMO ANALOGUE OF BLEBBISTATIN (SCHEME 5) 44

4.4 RESULTS AND DISCUSSION 48

5 CONCLUSION 49

6 REFERENCES 50

1 ABRREVIATIONS

ADP	adenosine diphosphate
ATP	adenosine triphosphate
ATPase	adenosine triphosphatase
BDM	2,3-butanedione monoxime
BTS	*N*-benzyl-*p*-toluene sulfonamide
DCM	dichloromethane
DMA	dimethylacetamide
DMSO	dimethyl sulfoxide
ee	enantiomeric excess
EtOAc	ethyl acetate
GFP	green fluorescent protein
HPLC	high-performance liquid chromatography
IC_{50}	half maximal inhibitory concentration
LRMS	low resolution mass spectrometry
MeOH	methanol
$MgSO_4$	magnesium sulphate
MHC	myosin heavy chain
MLC	myosin light chain
MTBE	methyl *tert*-butyl ether
NMII	non-muscle myosin II
PBP	pentabromopseudilin
PClP	pentachloropseudilin
PE	petroleum ether

Pi	inorganic phosphate
$POCl_3$	phosphoryl chloride
RNA	ribonucleic acid
RT	room temperature
SAR	structure-activity relationship
Tf_2O	trifluoromethanesulfonic anhydride
THF	tetrahydrofuran

2 AIM OF THE WORK

The aim of this work is to design and prepare novel blebbistatin derivatives as potential myosin inhibitors with enhanced or modified properties compare to original compound based on structural research of already reported blebbistatin analogues.

Additionally, another goal is to optimize and find alternative methods for an amidine synthesis, which is a low-yielded reaction in (*S*)-blebbistatin synthesis in order to get better yields as well as suggest a different synthetic strategy that allows for easier access to novel blebbistatin derivatives.

3 THEORETICAL PART

3.1 MYOSIN SUPERFAMILY

3.1.1 INTRODUCTION OF MYOSINS

Myosin superfamily is a large and diverse group of ATP-dependent actin-based motor proteins, which are involved in several cellular processes such as muscle contraction, cytokinesis, organelle transport, cell polarization, apoptosis, phagocytosis, exocytosis and signal transduction.[1- 4]

Based on phylogenetic analyses of conserved structural domains this superfamily can be divided into at least twenty four classes (Figure 1). Twelve of these classes are expressed in mammalian cells (I-III, V-VII, IX, X, XV, XVI, XVII, and XIX).[2,3]

Particular myosins occur in different organs or cell types based on their structural and functional characteristics. The first described myosin was isolated from the muscle cells, now denoted as muscle myosin II. Nevertheless, the majority of the members of the myosin superfamily are non-muscle myosins, so called unconventional myosins abounding mainly in cytoplasm.

3.1.2 CONVENTIONAL MYOSINS

The myosin II class, also known as conventional myosins, is the most thoroughly studied and described class of myosin superfamily. As mentioned above, the first myosin was identified in muscle extracts by Willy Kühne in 1864.[1]

Besides muscle myosin II which is responsible for contraction of cardiac, skeletal and smooth muscles, there is the other member of this class, which is present in all non-muscle eukaryotic cells – non-muscle myosin II (NMII). This myosin is involved in cell adhesion, division and migration. Paradoxically, NMII also occurs in muscle cells, where it fulfils distinct functions in the process of skeletal muscle development and differentiation, as well as sustention of tension in smooth muscles.[5]

One of the structural hallmarks for this class is a dimeric unit able to form thick filaments.

3.1.3 UNCONVENTIONAL MYOSINS

Unconventional myosins is a group of relatively recently discovered motor proteins, which can be monomeric or dimeric, but compared to conventional myosins, it

is assumed that they are not able to form filaments.[6] For better understanding of the topic, a brief introduction of several the most important members of this group has been done below.

Myosin I was the first described unconventional myosin. It can be found in *Acanthamoeba*, *Dictyostelium*, *Saccharomyces*, *Emiricella* (*Aspergillus*), chicken, mice, rats and humans. The members of this class are monomers divided into four subclasses. Their functioning influences processes such as cell crawling, chemotaxis, phagocytosis or cell division.[7]

Myosin III was firstly isolated from *Drosophila* eye. Further, it can be found in horseshoe crabs, fish and humans. The function of this class is involved in phototransduction.[7]

Myosin V has been identified in *Drosophila*, *Caenorhabditis elegans*, yeast, chicken, rats and humans.[6] This class of myosins has an important role in cargo transport, such as organelle, vesicle and RNA transport. Furthermore, it may be involved in chromosomal segregation, acrosome formation and nuclear morphogenesis during the process of spermatogenesis.[3]

Myosin VI has been found in *Drosophila*, *Caenorhabditis elegans*, pigs, mice, chicken and humans. This class of myosins is presumably responsible for anchoring of stereocilia rootlets.[8]

Myosin VII occurs in *Drosophila*, *Caenorhabditis elegans*, mice, pigs and humans. Two types of this myosin have been described so far, VIIA and VIIB. Very little is known about the function of myosin VII. More studied myosin VIIA is involved in stereocilia integrity and in membrane trafficking in the inner ear hair cells.[8]

Myosin VIII, XI and XIII have been identified in higher plants. Several studies confirmed that these classes of plant myosins play a significant role in organelle movements.[9]

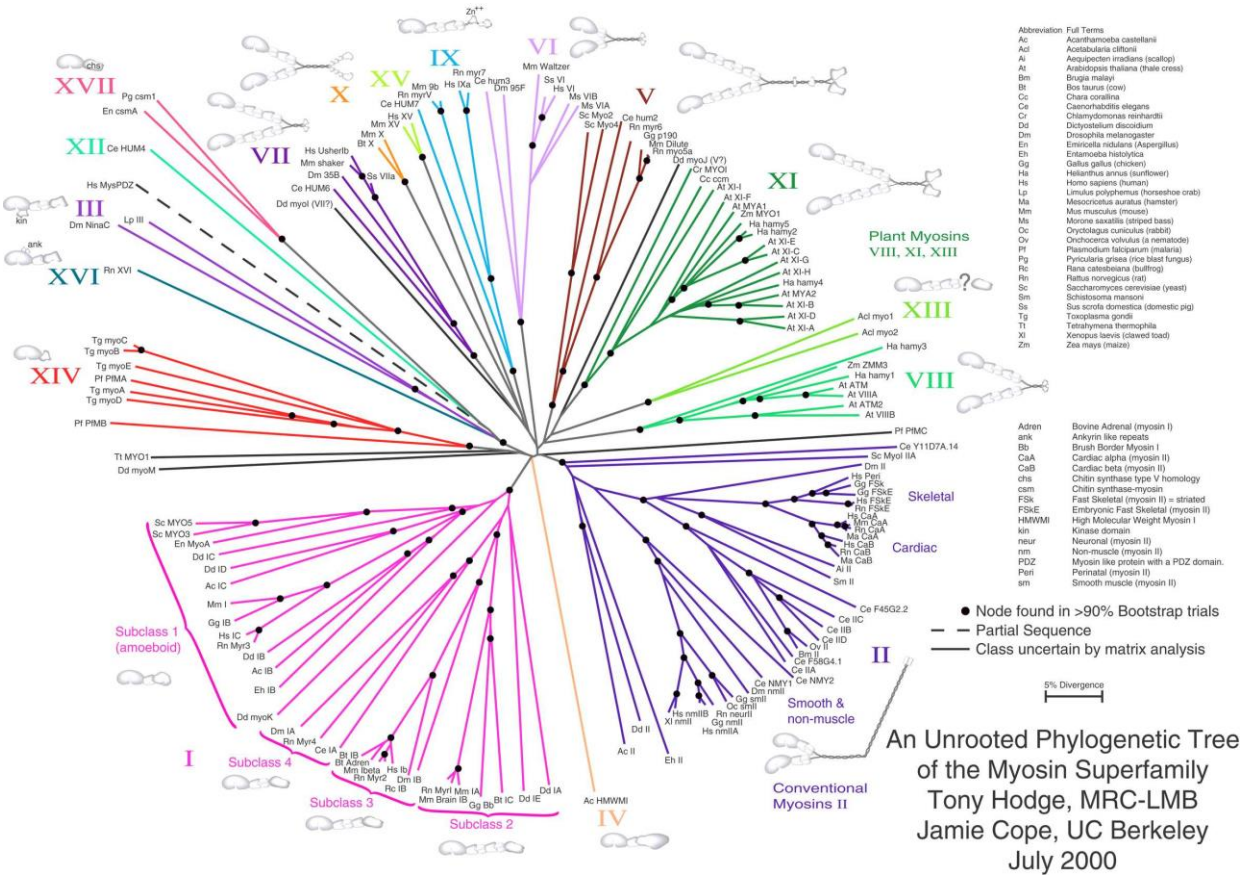

Figure 1. Myosin superfamily tree based on phylogenetic analyses. *(Taken up from reference* [10]*)*

3.1.4 MYOSIN STRUCTURE

Generally, all myosins are composed of one or two heavy chains, forming the basic structure of the protein, and several light chains, having a modulatory and regulatory functions. The heavy chains are organized into three structurally and functionally different domains[4] (Figure 2):

- *N*-terminal head (motor) domain containing actin-binding regions as well as Mg^{2+} ATPase site. This head domain is the most conserved region among the myosin superfamily and is responsible for force generation.
- Central α-helical neck or lever-arm region, which binds to modulatory light chains or calmodulin. This region increases smaller movements within the catalytic domain during the chemo-mechanical ATPase cycle.
- *C*-terminal tail domain mediating cargo-binding and intracellular targeting. This domain usually possesses a coiled coil region.[3,4]

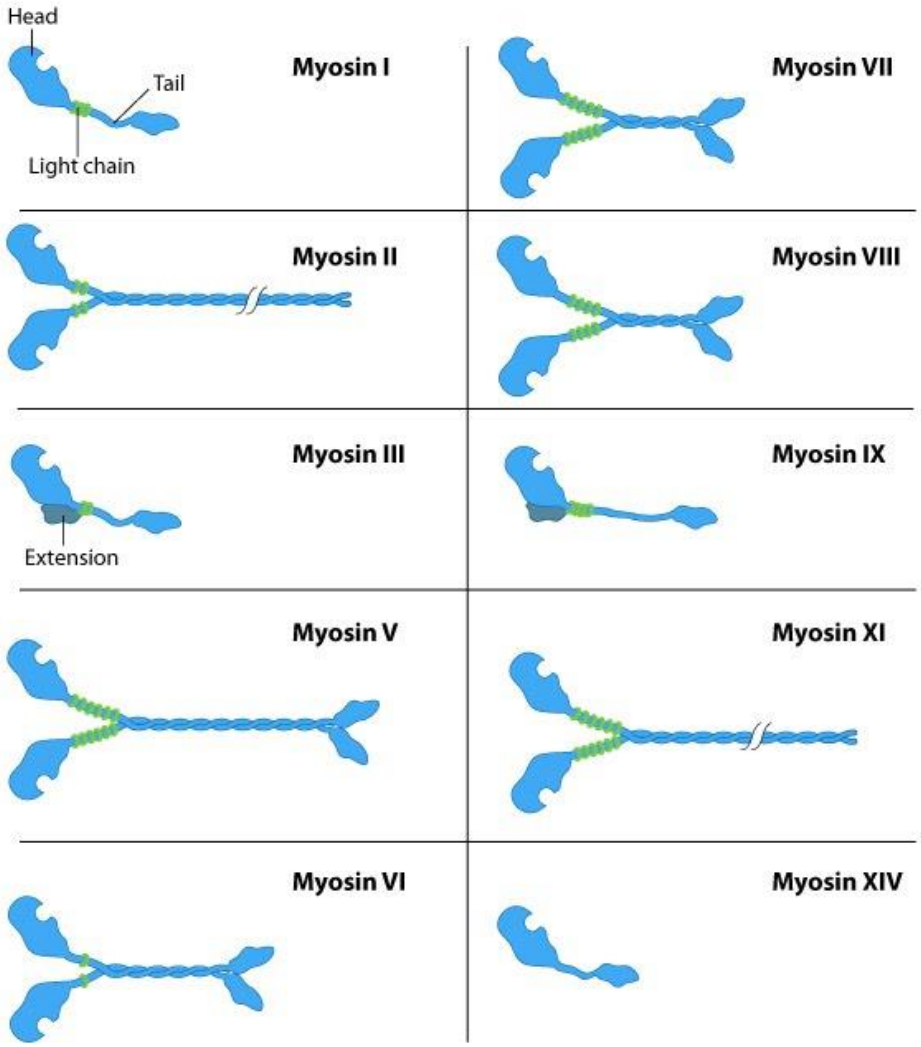

Figure 2. Myosin structures. *(Taken up from reference* [11]*)*

3.1.5 MOLECULAR MECHANISM – ATPASE CYCLE

Movement of myosin along the actin filament requires energy, which is obtained by hydrolysis of ATP by actin-activated ATPase in the motor domain. This process can be described in several steps (Figure 3).

Myosin free of ATP binds tightly to actin in "rigor" state. Binding of ATP to myosin causes conformational change resulting in dissociation of the myosin motor from actin. In this phase myosin repositions itself into a "cocked" state and hydrolyzes ATP to ADP and inorganic phosphate (Pi). Thereafter, stable myosin-ADP-Pi intermediate forms. Such intermediate rebinds actin and releases inorganic phosphate, which triggers the myosin "power stroke" resulting in motor movement along actin. Subsequently, ADP

is released and myosin forms the actomyosin “rigor” state ready to start the ATPase cycle again.[2] It is noteworthy that myosin head walks toward the (+)-end of actin filament.

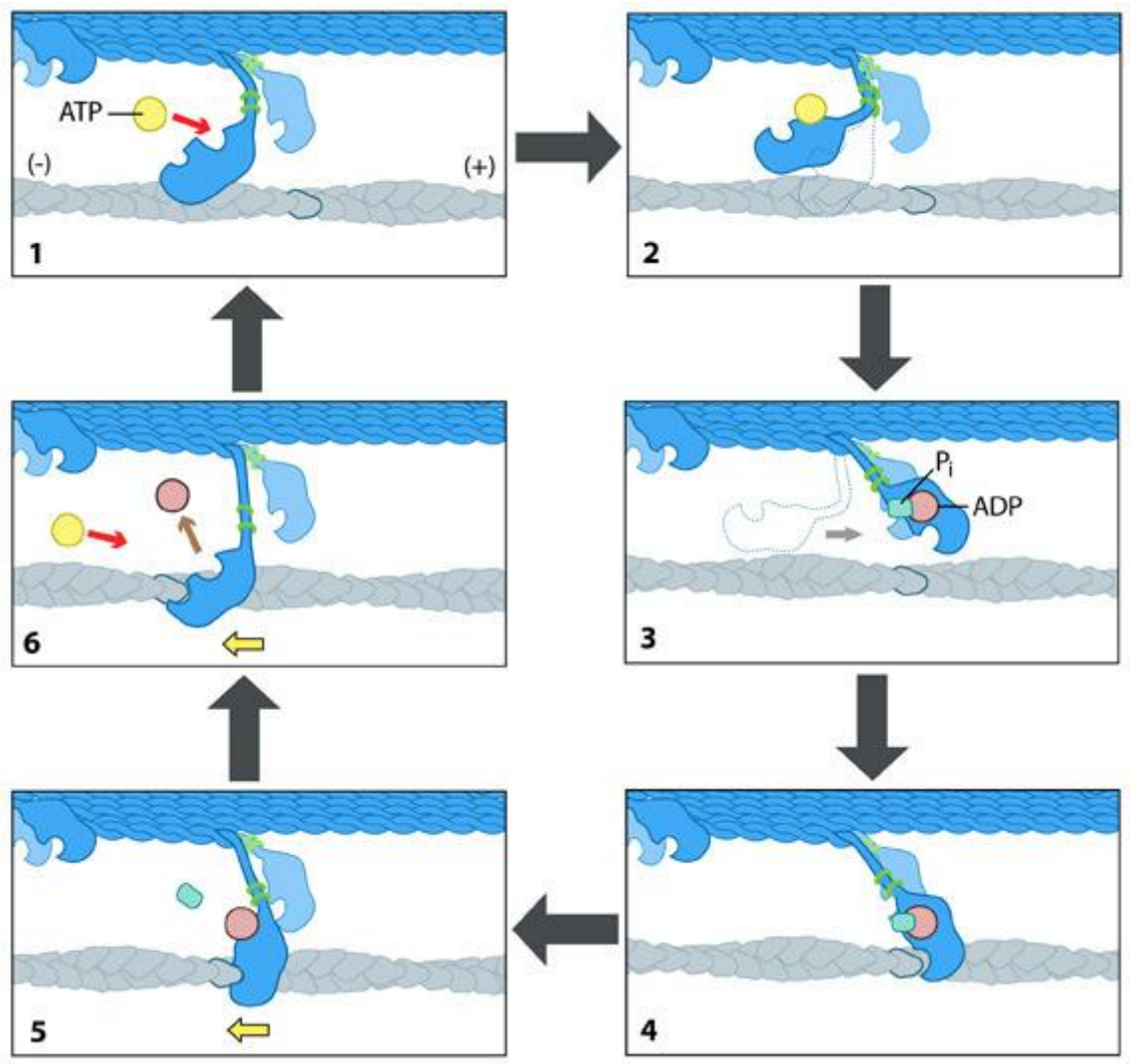

Figure 3. ATPase cycle of myosin motors. *(Taken up from reference* [12]*)*

3.1.6 REGULATION OF MYOSIN ACTIVITY

There are many possibilities to regulate the activity of myosins leading to changes in processes such as cell adhesion, polarity of migrating cells, morphogenesis and many other functions that myosins are involved in.[5]

Generally, the simplest way how to regulate the myosin activity is phosphorylation of myosin chains, both myosin heavy chains (MHC) and myosin light chains (MLC). This phosphorylation is provided by a network of kinases.

Dozens of diverse kinases able to phosphorylate the MLCs have been discovered, e.g. myosin light chain kinase, coiled coil-containing kinase, citron kinase, leucine zipper interacting kinase.[5] The main difference between these kinases is their mode of activation and their localization in cells.

Myosin II assembles into filaments. Phosphorylation of its MHCs causes changes in electrostatic interactions between particular MHCs leading to disruption of myosin filaments[13] or prevention of their formation[5]. Among the kinases able to phosphorylate the heavy chains belong calmodulin kinase II, casein kinase II and the members of the protein kinase C family.[13]

It is also worthy to mention a metastasis-associated protein S100A4, also known as MTs1, which directly binds the MHC IIA isoform and thus prevents filaments formation. Such interaction may affect cell polarization and membrane protrusion, which can increase cell migration and tumor metastasis.[13]

3.1.7 DISEASES ASSOCIATED WITH MYOSIN MUTATIONS AND DYSFUNCTIONS

It has been found that myosins are linked to several human diseases and genetic syndromes. For example, myosin VIIA mutations lead to non-syndromic deafness or Usher syndrome resulting in hearing loss and blindness.[1] Myosin VA mutation is connected to Griscelli syndrome, which is characterized by hypopigmentation and immunodeficiency.[1] Dysfunction of cardiac myosin II and myosin VI is involved in hypertrophic cardiomyopathy[2], and mutation of non-muscle myosin II can cause deafness[1].

Last but not least, non-muscle myosins have been also implicated in cancer. Based on their cellular functions they can be either tumor progressive or suppressive.[14]

Therefore, the development of small molecule myosin activators or inhibitors represents a great potential in order to help us to understand the mechanisms of such diseases or even to improve their treatment.

3.2 INHIBITORS OF MYOSIN

Generally, there are two types of inhibitors of protein kinases – competitive and uncompetitive. In myosin case, competitive inhibitors have several disadvantages, such as lack of selectivity (can also inhibit non-myosin ATPases) and furthermore, myosins

blocked by competitive ATPase inhibitors remain bound to actin thus physically impeding non-inhibited myosins to bind this actin site.

Based on abovementioned findings, uncompetitive myosin inhibitors represent greater potential as they bind to the protein at the allosteric site outside the ATP binding pocket thus having no secondary effect on other ATPases/ATP-binding proteins.

Among uncompetitive myosin inhibitors belong, for example, pentachloropseudilin (PClP), pentabromopseudilin (PBP), myoVin-1, *N*-benzyl-*p*-toluene sulfonamide (BTS) or 2,3-butanedione monoxime (BDM). PClP, inhibitor of myosin I, is highly halogenated natural antibiotic and it affects enzyme by reducing coupling between actin and nucleotide-biding sites. In addition, PClP also inhibits myosin V and NMII at higher concentrations (IC_{50} > 90 μM). Another member of pseudilin family having similar properties as PClP is PBP isolated from *Pseudomonas bromoutilis.* PBP exhibits higher affinity to myosin V and moreover, besides the same mechanism of inhibition as PClP, it also reduces ADP dissociation, ATP binding and hydrolysis. Inhibitor of myosin V - myoVin-1, the pyrazolopyrimidine-based compound, hinders ADP release from a protein. BTS is an aryl sulfonamide derivative exhibiting high affinity to fast-twitch skeletal muscle myosin at the same time impeding both release of Pi and ADP. BDM, originally synthetized as acetylcholinesterase reactivator, is able to inhibit muscle contraction by affecting skeletal myosin II in the step of Pi dissociation.[2] Last but not least, the most well-known and widely used uncompetitive inhibitor of myosin is blebbistatin. This derivative of 1-phenyl-1,2,3,3a-tetrahydro-4*H*-pyrrolo[2,3-*b*]quinolin-4-one blocks myosin II activity by hindering the release of Pi from the myosin-ADP-Pi complex.[15] The graphical overview of mechanisms of aforementioned inhibitors is depicted in Figure 4 and Figure 5.

The main focus of present work is characterization of blebbistatin and its derivatives as well as design and synthesis of novel entities.

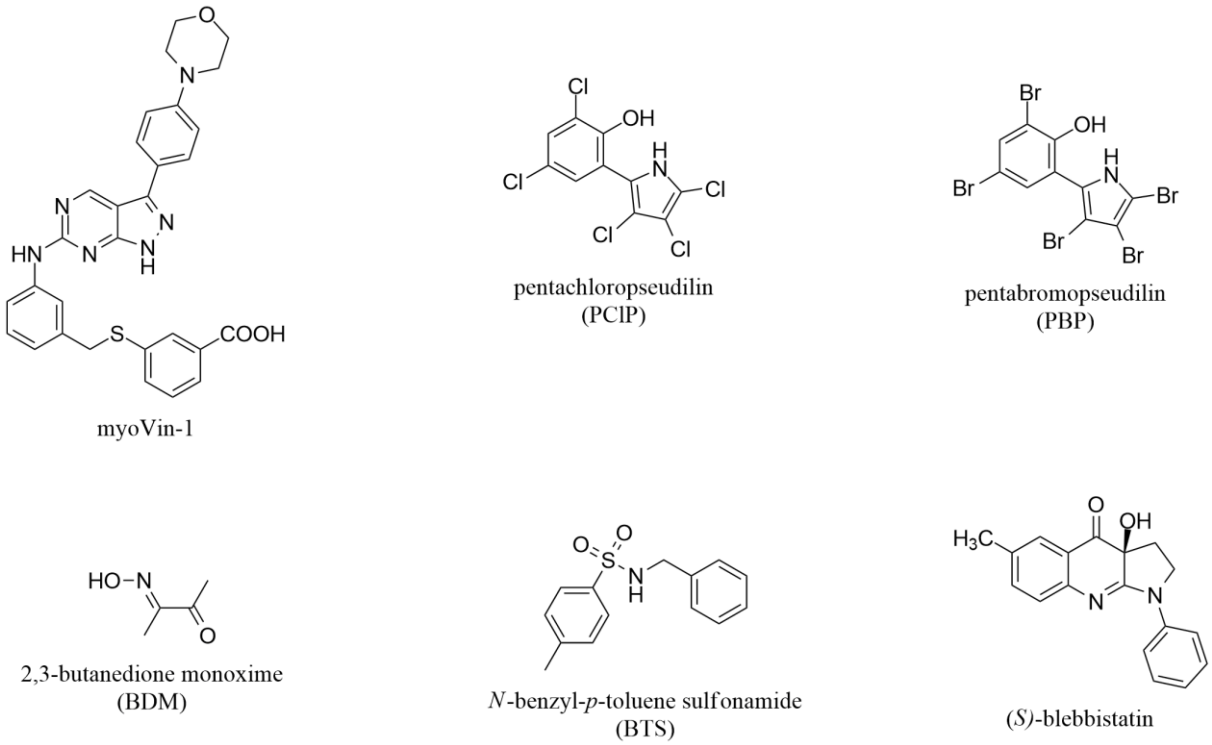

Figure 4. Inhibitors of myosin.

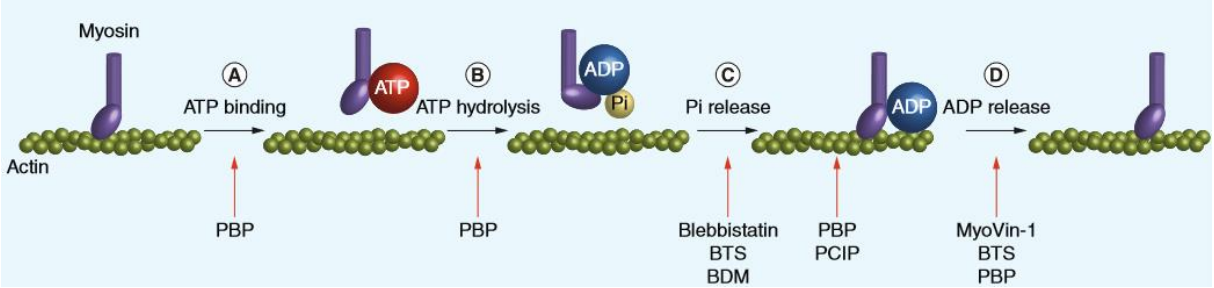

Figure 5. Inhibition mechanism of myosin inhibitors. BDM: 2,3-butanedione monoxime; BTS: *N*-benzyl-*p*-toluene sulfonamide; PClP: pentachloropseudilin, PBP: pentabromopseudilin. *(Taken up from reference* [2]*)*

3.3 BLEBBISTATIN

3.3.1 INTRODUCTION OF (*S*)-BLEBBISTATIN

As mentioned above, (*S*)-blebbistatin (Figure 6) is an uncompetitive inhibitor of non-muscle myosin II discovered by a high-throughput screening.[16] Additionally, it has been revealed that blebbistatin itself is a degradation product of the "aged" DMSO solution of azatacrine analogue, which does not exert inhibition activity towards non-muscle myosin II.[17]

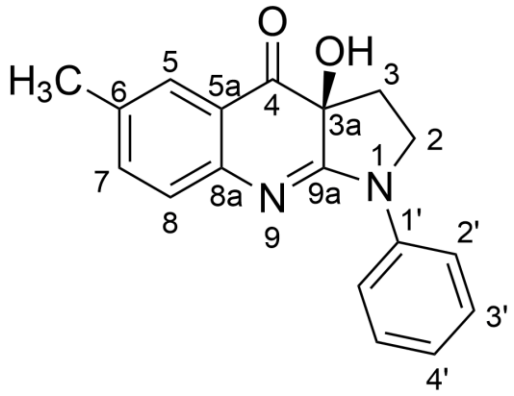

Figure 6. (*S*)-Blebbistatin.

The name of the compound was derived from its ability to inhibit formation of cell blebs. Bleb is a protrusion or flexure of the cytoplasmic membrane caused by disconnection of cytoskeleton from the membrane. This process, also designated as blebbing, appears, for example, during apoptosis. Moreover, (*S*)-blebbistatin rapidly disrupts cell migration and cytokinesis as well as cleavage of furrow ingression, but it does not affect an assembly of cleavage furrow.[16]

(*S*)-Blebbistatin has become a significant small molecule tool for studying of the myosin properties and functions in cell processes. Comparing to classical genetics and RNAi technology studies it has a huge advantage in the ability to reversibly control the activity of a protein (by washing it in or out). Other general advantages of small molecules are, for instance, easy application to cross-species studies, possibility of administration of the combination of small molecules, excellent temporal resolution, study of the function of essential or recessive genes and many others.[18] In addition, these selective and high affinity compounds principally do not interfere with other cellular processes.

3.3.2 MECHANISM OF MYOSIN INHIBITION BY BLEBBISTATIN

(*S*)-Blebbistatin inhibits NMII, as well as skeletal myosin II, exerting at the same time no effect on smooth muscle myosin II or myosins of other classes.[15]

(*S*)-Blebbistatin binds to a motor domain of myosin, in particular to a hydrophobic pocket at the apex of the 50kDa cleft and does not compete with substrate for nucleotide binding sites.[19] As mentioned above, in the process of ATPase-cycle the motor domain of enzyme occurs in several conformational forms. The mechanism of inhibition consists in binding of blebbistatin to myosin-ADP-Pi intermediate (detached from actin filament)

resulting in a specific perturbation in the nucleotide binding pocket and stabilization of this complex.[15] Finally, the release of inorganic phosphate (Pi) is inhibited and evoking associated myosin power stroke, thus the myosin is not able to bind to actin filament to form a "rigor" state again (Figure 5).

3.3.3 STRUCTURAL BASIS OF MYOSIN INHIBITION BY BLEBBISTATIN

Although the blebbistatin binding pocket in myosin motor domain is one of the most conserved segments among the myosin superfamily, the slightest sequence and structural changes in this region give blebbistatin the ability to distinguish among myosin isoforms.[19] Therefore, it is very important to know, how blebbistatin interacts with the myosin.

Allingham and co-workers have studied the binding mode of blebbistatin to *Dictyostelium discoideum* myosin II and they have revealed that it is controlled by the hydrophobic interactions.[20] The benzyl ring of (*S*)-blebbistatin is enveloped by the side chains of Leu262, Phe466, Glu467 and Val630, while the tetrahydropyrrolo ring and the oxo group interact with Ser456 and Ile471. The methylquinolinone moiety is clustered by Tyr261, Thr474, Tyr634, Gln637 and Leu641 (Figure 7).[20]

Furthermore, it has been investigated how the sequence and structural differences of diverse myosins correlate with the level of inhibition by blebbistatin. Indeed, comparison of the homologous residues of rabbit skeletal muscle myosin II, non-muscle myosin IIB to those in *D. discoideum* myosin II, disclosed that Ser456, Thr474, Tyr634 and Gln637 residues exert many variabilities among the myosin isoforms, thus influencing blebbistatin inhibition.[20]

Moreover, the enantioselectivity for (*S*)-stereoisomer is explained by a formation of hydrogen bonds between the chiral hydroxy group of blebbistatin and Leu262 or Gly240. (*R*)-stereoisomer is not able to form such interactions thus exerting lower affinity to myosin.[20]

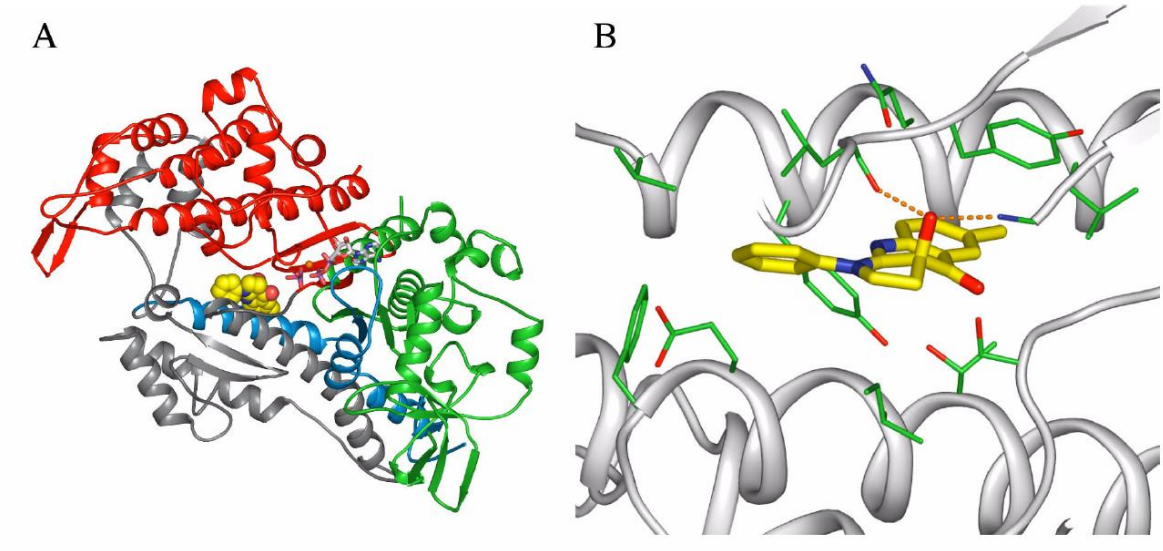

Figure 7. A) (*S*)-Blebbistatin bound to *D. discoideum* myosin II. **B)** The blebbistatin-myosin binding site. Selected amino acid residues interacting with blebbistatin are displayed in green sticks representation.[20] *(Taken up from reference* [20]*)*

In order to better understand structure-activity relationship of blebbistatin Lucas-Lopez's group synthetized a series of blebbistatin analogues differing in the position of methyl group of the quinolinone part (Figure 8).[19] Other SAR study investigated an impact of oxo and hydroxy functional groups on inhibitory activity of blebbistatin.[21] Based on the results of these studies, several findings can be deduced. The positioning of the methyl group at C5, C6, C7 or its absence still allows the molecule to fit in the 50kDA cleft of myosin II and keep its inhibition activity. On the other hand, methyl incorporation into C8 position hinders the compound to remain in the hydrophobic pocket, so such derivative has no effect on activity. In addition, it has been confirmed that conservation of oxo functional group at C4 and keeping the stereochemistry of the C3a chiral center are one of the essential factors for retaining its biological activity. Last but not least, the aromatic quinolinone moiety and the phenyl ring are essential as well for maintaining the inhibitory activity.[19,21]

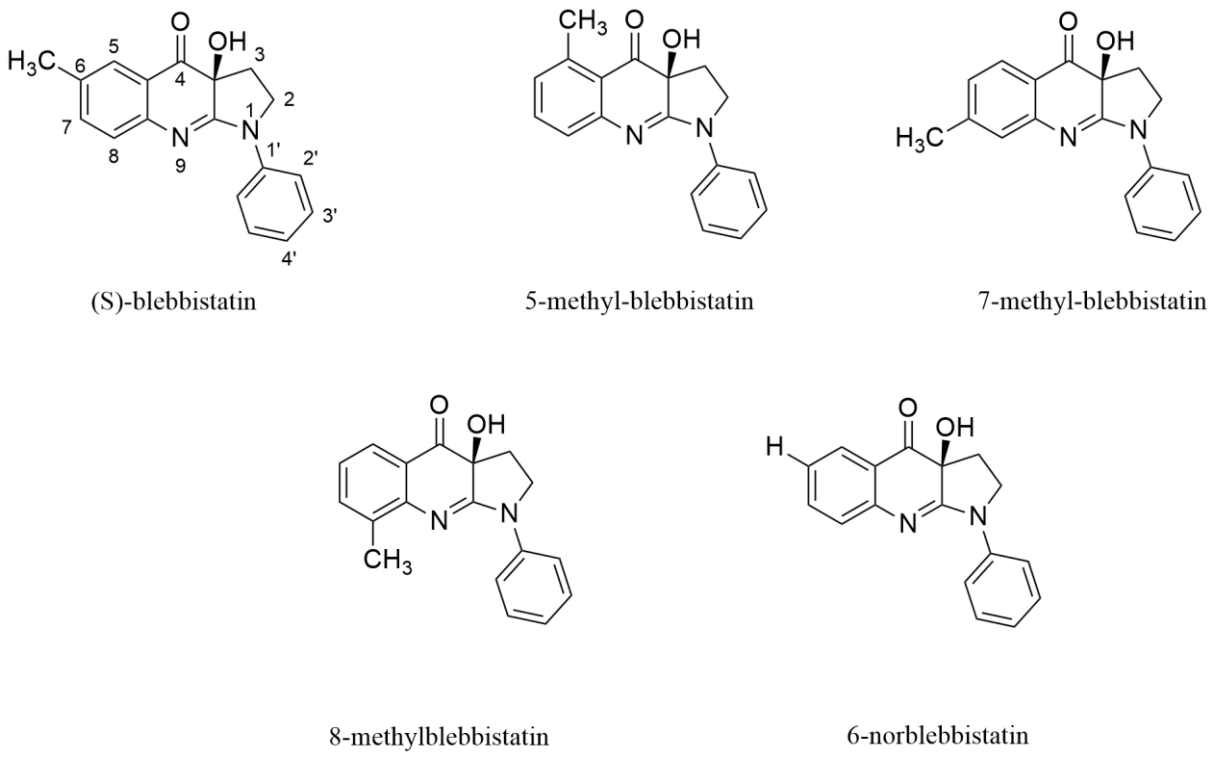

Figure 8. (*S*)-Blebbistatin and its positional methyl analogues and demethylated derivative.

These structure modifications also revealed that several analogues resulted in much higher selectivity among non-muscle myosin II isoforms, i.e. NMIIA (human), NMIIB (human), NMIIC (mouse).[21] Therefore an interesting direction in blebbistatin derivatives development has been uncovered, which can lead to discovery of even more potent and selective compounds than blebbistatin.

3.3.4 PROS AND CONS OF (*S*)-BLEBBISTATIN

As mentioned above, (*S*)-blebbistatin has many advantageous factors, such as possibility of reversible myosin inhibition by washing it out. Further, it was also confirmed that blebbistatin is a specific inhibitor of myosin class II, and that it does not inhibit any other myosin classes such as I, V, X or XV.[18] The inhibitory effect towards myosin ATPase of the compound was assessed by determination of its IC_{50} value which ranges in 0.5–5 μM.[16]

Despite undoubted advantages of (*S*)-blebbistatin, there are also several limitations in its usage. For a purpose of study of protein distribution and function within a cell, the fluorescence microscopy techniques are usually performed. These experiments are very often based on green fluorescent protein (GFP) fusion with the investigated

protein. Thanks to GFP, proteins can be easily visualized by irradiation with light of wavelength 420–490 nm and consecutive collection of emitted light from the investigated protein.[18] Nevertheless, (*S*)-blebbistatin is fluorescent itself, as it exerts significant emission at 440 nm, which is in the GFP emission wavelength range. Therefore, usage of (*S*)-blebbistatin for the observations of the myosin functioning in live cells is limited, and it is necessary to perform these experiments by using an alternative fluorescent proteins (e.g. red fluorescent protein), which have different emission wavelength range. Furthermore, (*S*)-blebbistatin becomes phototoxic after prolonged exposure to the blue light (390–470 nm) resulting in degradation and generation of reactive oxygen species, which have not been identified so far.[22] Except light sensitivity of the compound, the other disadvantageous factor for biological studies is also the fact that after prolonged incubation in live cells blebbistatin has cytotoxic side effects even in the absence of irradiation.[23] Additionally, another limiting factor of the inhibitor is its low solubility in aqueous solutions.

Therefore, development of novel blebbistatin derivatives has great potential in order to eliminate these limitations and improve or modify its specific properties. Indeed, several blebbistatin derivatives, that have been synthetized by this time, confirm this effort to be worthy.

3.3.5 BLEBBISTATIN DERIVATIVES

To date, few interesting blebbistatin derivatives with enhanced or novel properties have been reported.

One of the directions in blebbistatin derivatives development is to improve their photostability compared to the reference molecule. It has been shown that introduction of nitro group into blebbistatin structure reduces the fluorescence emission in GFP wavelength range. In particular, it was a derivative synthetized by Patterson *et al.* – (*S*)-7-nitro-blebbistatin (Figure 9).[18] This led to further investigation and in 2014 Képiró's group introduced a photostable derivative – *p*-nitroblebbistatin (Figure 9).[23]

p-Nitroblebbistatin with a nitro group at C4′ position seems to be a good candidate for replacement of (*S*)-blebbistatin for the study of myosin II role in biological processes. It has been proven that C4′ nitro substitution of blebbistatin does not alter its biological activity, as the IC_{50} values of blebbistatin and *p*-nitroblebbistatin towards *D. discoideum* myosin II were almost the same (2.33 ± 0.13 μM and 2.96 ± 0.45 μM, respectively).

Comparing to (*S*)-blebbistatin, the C4′ nitro-substituted derivative is non-cytotoxic, non-phototoxic and non-fluorescence myosin II inhibitor. Thus *p*-nitroblebbistatin does not decompose upon blue light irradiation, its fluorescence is decreased by a hundred times and it does not affect the toxicity rate of the cells even after the 36 hours treatment with the compound. Therefore it can be claimed that (*S*)-blebbistatin can be adequately substituted by this derivative not only in biology within *in vitro* assays but also in treatment of human diseases.[23]

In response to positive results of *p*-nitroblebbistatin, chloro-derivative was also published. However, *p*-chloroblebbistatin (Figure 9), a derivative with chlorine at C4′ position, did not exert as good results as nitro-derivative. Nonetheless, thanks to this blebbistatin analogue it has been found out that improved photostability is not necessarily accompanied by reduced phototoxicity.[23]

Another interesting derivative is *p*-azidoblebbistatin (Figure 9), a derivative substituted at C4′ position by azido group also synthetized by Képiró and co-workers.[24] Besides similar inhibition properties as (*S*)-blebbistatin in conditions of the absence of UV irradiation, *p*-azidoblebbistatin forms covalently crosslinked complex with enzyme after the irradiation at 310 nm, non-toxic wavelength for cells and/or tissues. Therefore, this azido-derivative might be also considered as a novel tool with improved properties in structural studies of actomyosin contractility as well as in investigation of biological roles of myosin II.[24]

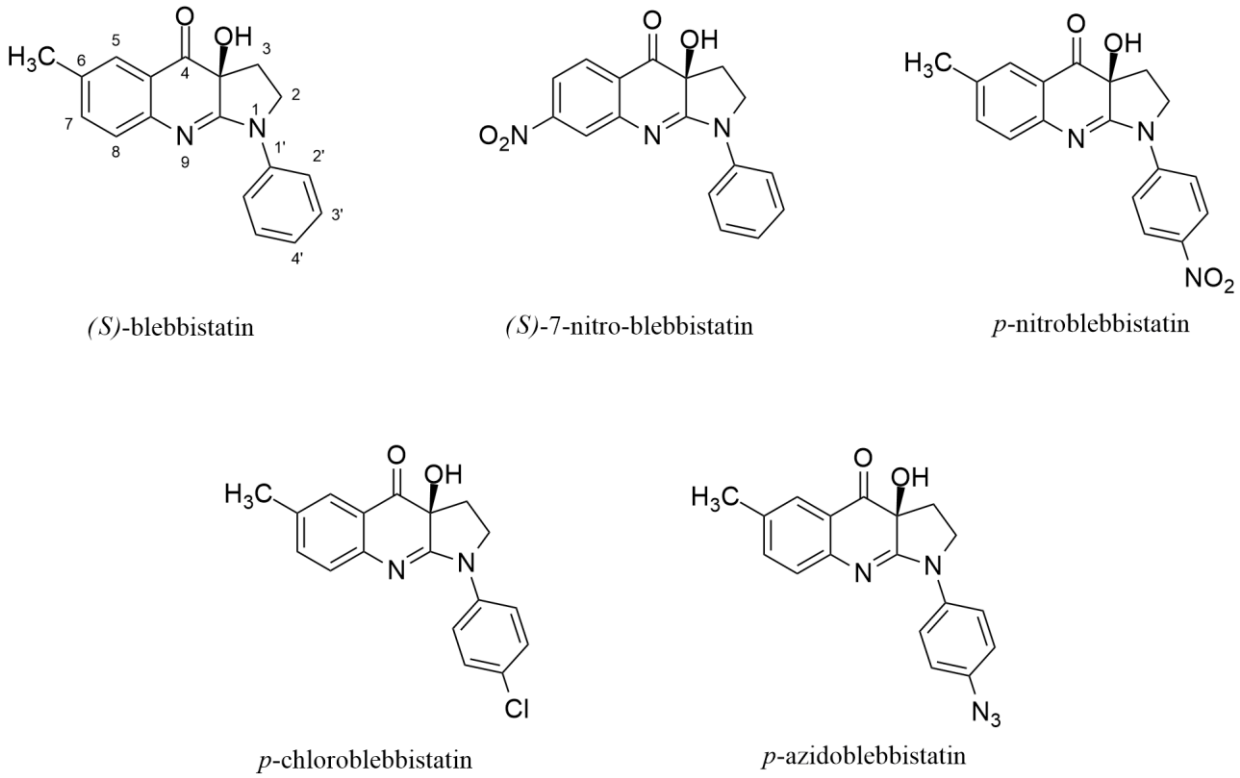

Figure 9. (*S*)-Blebbistatin and its derivatives.

4 EXPERIMENTAL PART

4.1 OPTIMIZATION OF BLEBBISTATIN SYNTHESIS

Current total synthesis of (*S*)-blebbistatin (**5**) (Scheme 1) published by Lucas-Lopez and co-workers has one big drawback – low yielding amidine synthesis (28%, compound **3**).[17] Such reaction exploits phosphoryl chloride ($POCl_3$) as an activator of *N*-phenyl-2-pyrrolidone (**2**). Therefore, one of the aims of this work was to investigate, suggest and develop an alternative synthesis of amidine intermediate in order to achieve higher yield of this step.

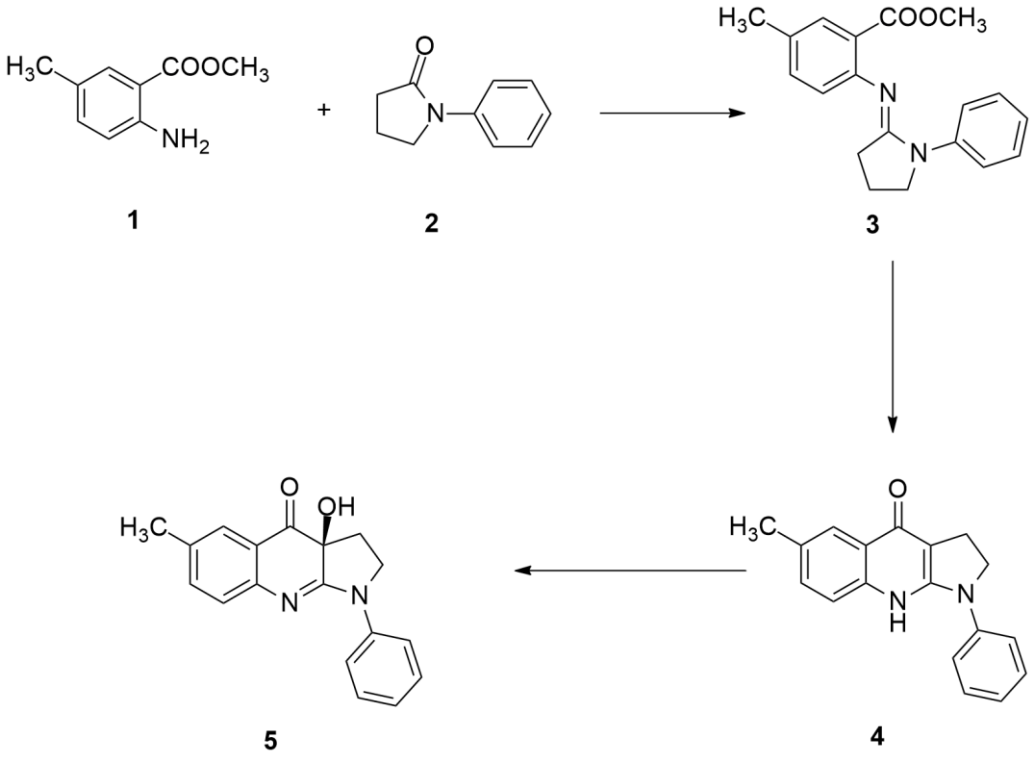

Scheme 1. Total synthesis of (*S*)-blebbistatin.[17]

To optimize this step (Scheme 2) we have decided to use methyl anthranilate (**6**) as a starting compound and to substitute phosphoryl chloride by trifluoromethanesulfonic anhydride (triflic anhydride, Tf_2O) supposing to be better activator of **2** than $POCl_3$.The reaction was pursued under different conditions, such as diverse reaction time or different reaction temperatures. Firstly, we have tried to activate amide with Tf_2O and pyridine according to the procedure described by Charette and Grenon[25] but unfortunately with no results even after changing the reaction conditions. Therefore, we have decided to change the protocol avoiding pyridine to let amide activate with Tf_2O only.[26] Such conditions bore the fruit in the form of desired intermediate (**7**). Unfortunately, according

to HPLC analysis the conversion was not complete, therefore there was no reason to use these conditions for amidine synthesis instead of current protocol with $POCl_3$. On the other hand, this can be still a hint for further investigation and development of more efficient amidine synthesis.

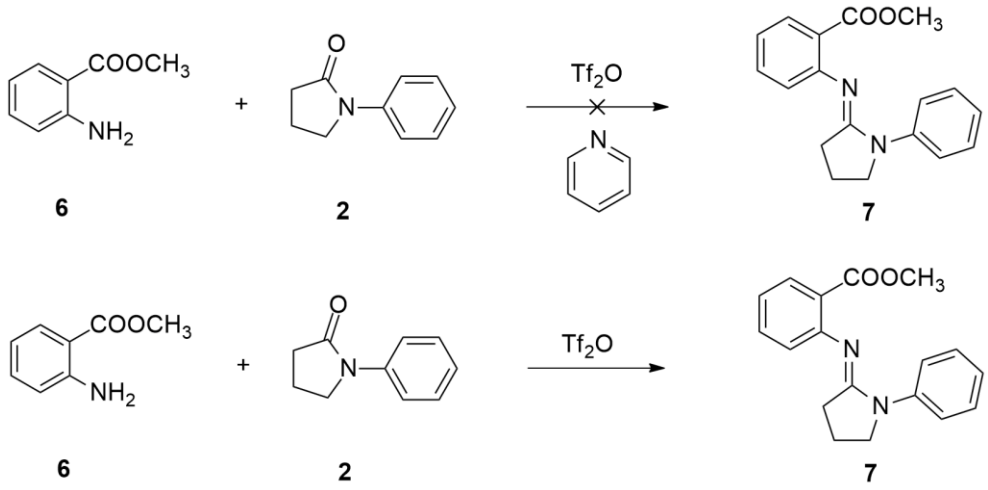

Scheme 2. Alternative amidine synthesis with triflic anhydride.

4.2 DESING OF NOVEL BLEBBISTATIN DERIVATIVES

According to structural and binding site studies as well as to properties of blebbistatin derivatives, it can be assumed that there is still a place for new blebbistatin derivatives with enhanced or modified properties including selectivity to particular myosin II isoforms.[18]

The best possibility for modification of (*S*)-blebbistatin (**5**) structure seems to be phenyl ring, but also quinolinone part, in particular at C6 or C7 position. As modifications of phenyl ring were studied by other groups, our task was to focus on quinolinone moiety of **5**. Last but not least aim of our work was to develop alternative synthetic strategy allowing easier synthesis of novel blebbistatin derivatives.

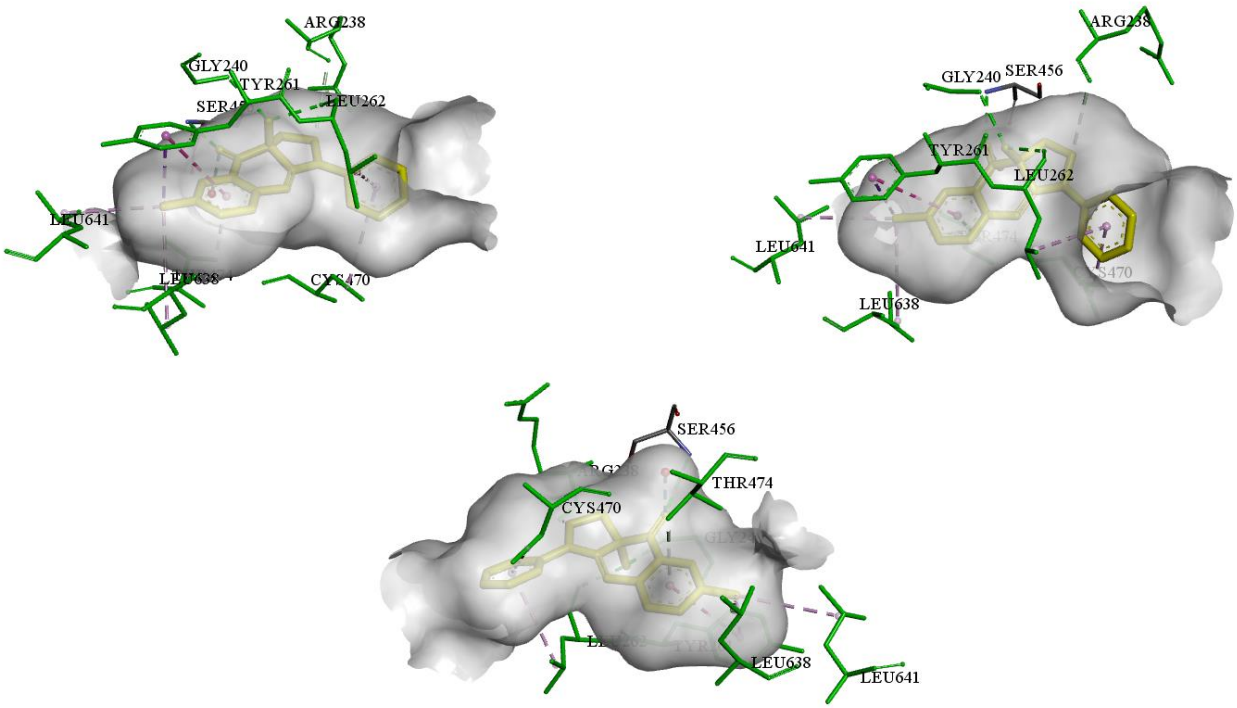

Figure 10. (*S*)-Blebbistatin binding site and its interaction with amino acid residues (displayed in green sticks representation) in 50kDa pocket of *D. discoideum* myosin II at different angles. *(Taken up from Protein Data Bank, accession code 1YV3, reference* [27]*).*

Generally, blebbistatin and its derivatives synthesis can be described in three basic steps, as depicted in Scheme 1. The first step has been already mentioned by formation of amidine intermediate. The second step exploits intramolecular Claisen-type condensation to form a quinolinone intermediate. In the last step, the quinolinone intermediate is stereoselectively oxidized by Davis oxaziridine to afford the final product. For reactions described below, stereoisomers (-)-(8,8-dichlorocamphorylsulfonyl)oxaziridine (**19**) and (+)-(8,8-dichlorocamphorylsulfonyl)oxaziridine (**20**) were used as Davis reagents prepared by K. Wagner (Figure 11).[28]

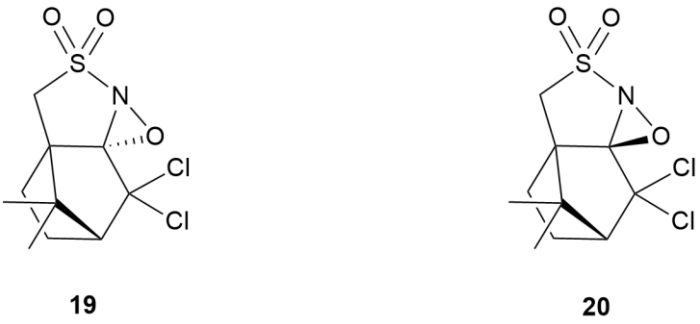

Figure 11. Davis oxaziridines. (-)-Davis oxaziridine (**19**), (+)-Davis oxaziridine (**20**). *These compounds were prepared by K. Wagner during his bachelor thesis research.*[28]

For know-how adoption already published analogue (*S*)-6-nor-blebbistatin (**9**) has been synthetized as well (Scheme 3).[19]

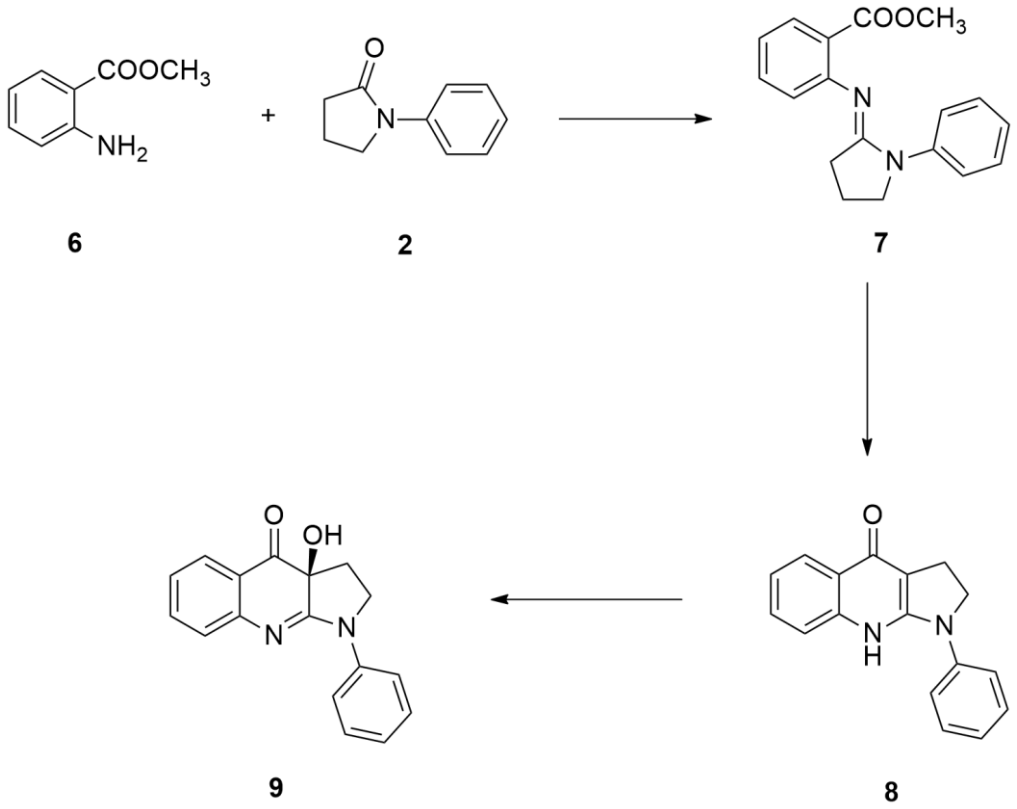

Scheme 3. Synthesis of (*S*)-6-nor-blebbistatin (**9**).

At first step of design of novel myosin II inhibitors, it was necessary to rationally propose their structures, respectively select potentially interesting functional groups that can be substituted at C6 position. The primary direction of such study was to prolong an alkyl chain at C6 position. Thus both enantiomers of 6-ethyl-blebbistatin (**16**, **17**) were prepared. The synthetic strategy consisted in development of an appropriate synthetic route which could be further applied in preparation of other blebbistatin derivatives at the

same time still using basic procedures from the total synthesis of (*S*)-blebbistatin. Thus the synthetic route yielding bromo-substituted intermediate (**13**) seemed to meet such requirements ().

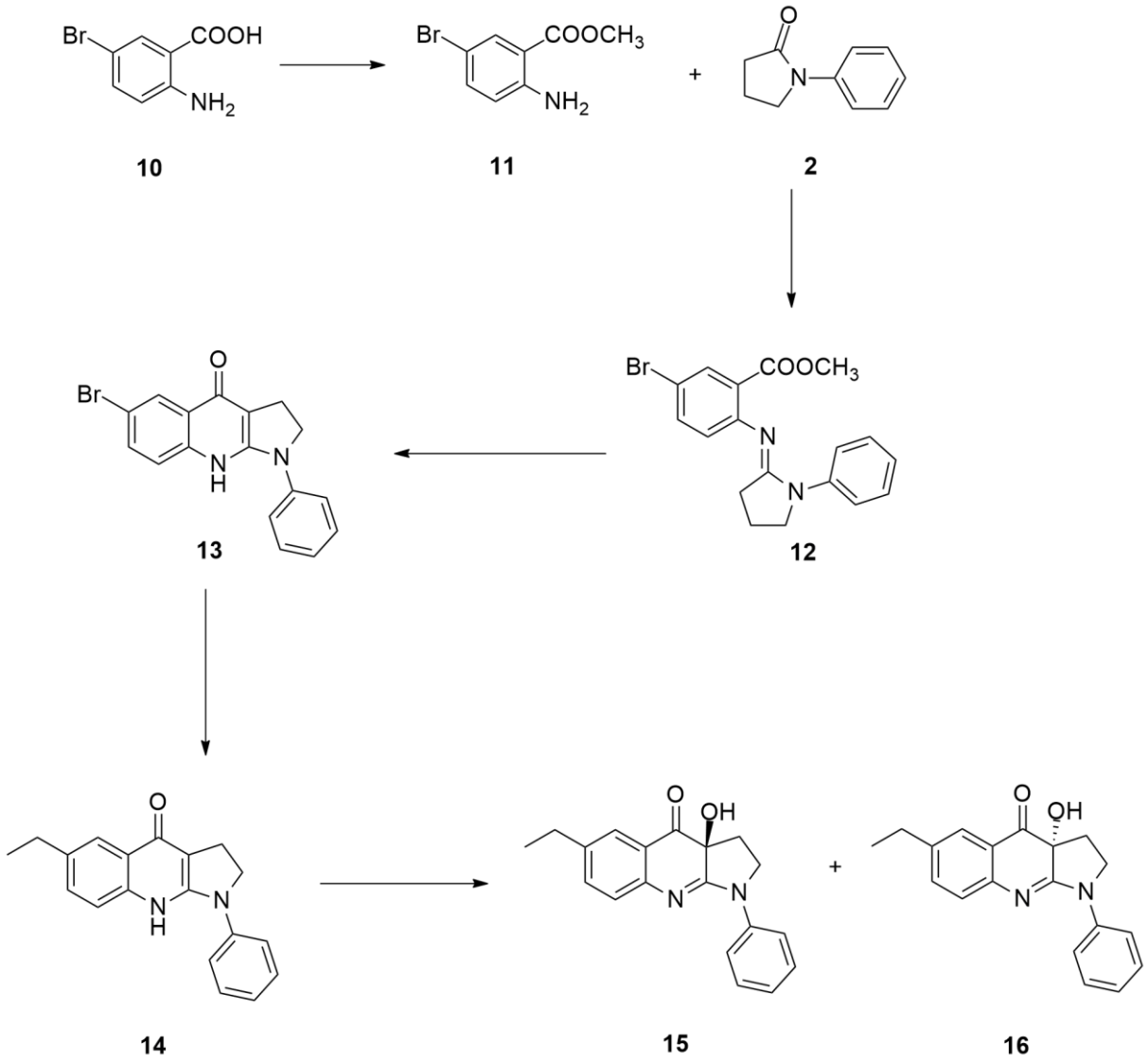

Scheme 4. Synthesis of ethyl-blebbistatin enantiomers.

Due to successful synthesis of intermediate **13** it was not also difficult to obtain bromo-substituted blebbistatin derivatives (**17**, **18**) (Scheme 5).

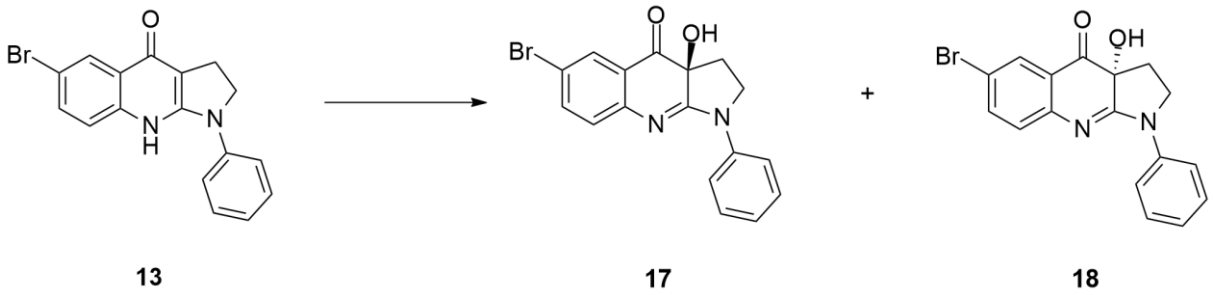

Scheme 5. Synthesis of bromo-blebbistatin derivatives.

Subsequently, we have focused on the synthesis of ethynyl analogues (**22**, **23**) (Scheme 6). Unfortunately, due to time deficiency, we did not manage to synthesize them.

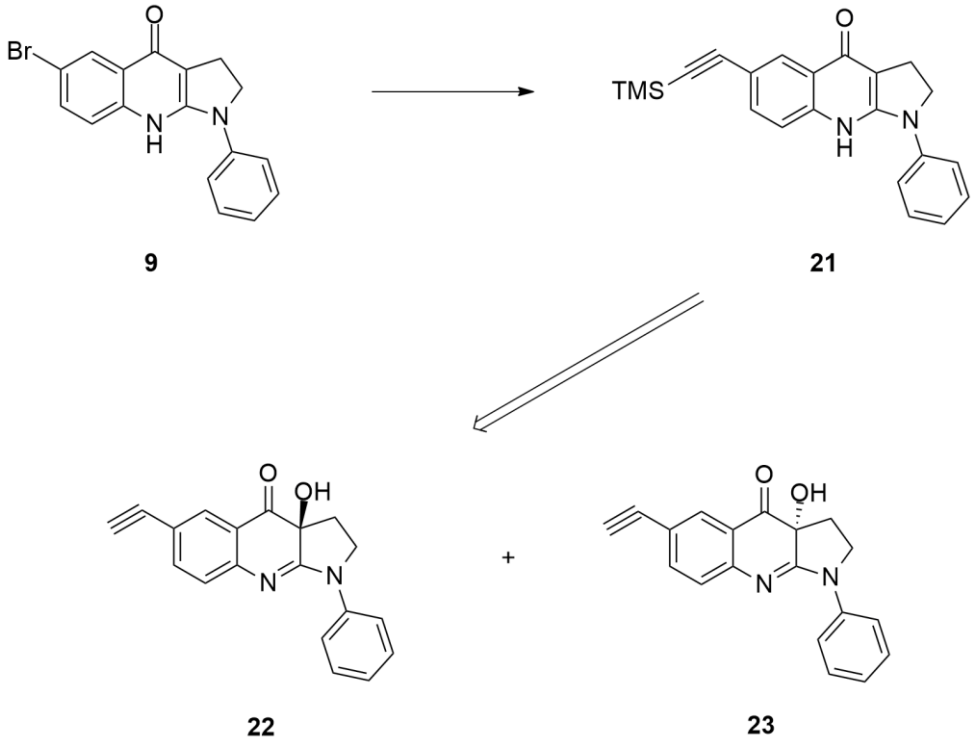

Scheme 6. Proposed synthesis of ethynyl-blebbistatin analogues.

4.3 SYNTHESIS OF NOVEL BLEBBISTATIN DERIVATIVES

Unless otherwise noted, starting materials and reagents were obtained from commercial suppliers and were used without further purification.

All reactions were performed in flame dried glassware under protective atmosphere (N_2 or Ar) if not stated otherwise.

Analytical thin layer chromatography (TLC) was performed on Merck silica gel 60 F_{254} supported on aluminum sheets; compounds were visualized using irradiation with ultraviolet light at 254 nm and/or 366 nm and/or by using the following staining solution (dip, dry & heat development). Staining solution: $KMnO_4$ (1 g), K_2CO_3 (6.6 g), 5% NaOH (1.7 mL) in H_2O (90 mL).

Chromatographic separation was performed by flash column chromatography on silica gel 60 (40 – 63 µm, Merck) (approx. 0.3 bar positive pressure).

Nuclear magnetic resonance (NMR) spectra were recorded on the following instruments: Bruker Avance I 250 (250/63 MHz), Bruker Fourier 300 (300/75 MHz), Bruker Avance I 400 (400/101 MHz) and Bruker Avance III 400 (400/101 MHz, *Z*-gradient broad band observe or inverse probe). Chemical shifts (δ) are expressed in parts per million (ppm) with respect to the solvent signal ($CDCl_3$-*d*, MeOH-d_4, DMSO-d_6) and spin multiplicities are given as s (singlet), bs (broad singlet), d (doublet), dd (doublet of doublets), t (triplet), q (quartet, p (pentet) or m (multiplet).

LC-coupled electrospray mass spectrometric analyses (LRMS, ESI-MS) were performed on a Finnigan LCQ spectrometer operating in positive or negative ion mode. Calculated masses were obtained using the software ChemDraw Ultra (CambridgeSoft Corporation) or Xcalibur.

HPLC analyses (achiral stationary phase: EC 125/4 Nucleodur C_{18} gravity, 5 µm, Macherey-Nagel) were conducted on a combined Shimadzu system (components: LC-10AT, DGU-14A, SIL-10AD, SCL-10A, LC-10AT, CTO-10AC, SPD-M20A, SPD-10A) using acetonitrile/water mixtures as mobile phase with a flow rate of 1 mL/min and detection at wavelengths of 203, 220 and 254 nm. The following gradients (MeCN:H_2O) were employed: Method A: 50:50 → 95:5 in 10 min, 95:5 for 20 min; Method B 10:90 → 95:5 in 15 min, 95:5 for 15 min.

Chiral HPLC analyses were conducted on a combined Shimadzu system (components: LC-10AT, DGU-14A, SIL-10AD, SCL-10A, LC-10AT, CTO-10AC, SPD-M20A, SPD-10A) using a Daicel Chiralpak IA (5 µm, 250/4.6) as chiral stationary phase, isocratic *n*-hexane/ethanol mixtures (ratio see compound data) as mobile phase with a flow rate of 1 mL/min and detection at wavelengths of 203, 220 and 254 nm.

For melting point determination a Büchi B-545 melting point apparatus and open capillaries were used.

4.3.1 SYNTHESIS OF (*S*)-6-NOR-BLEBBISTATIN (SCHEME 3)

Methyl 2-[*(E)*-(1-phenylpyrrolidin-2-ylidene)amino]benzoate (7)

To the solution of *N*-phenyl-2-pyrrolidone (**2**, 0.16 g, 1.0 mmol) in DCM (1 mL) phosphoryl chloride (101 μL, 1.1 mmol) was added dropwise and stirred at RT for 3 h. Then solution of methyl anthranilate (**6**, 0.15 mg, 1.0 mmol) in DCM (4 mL) was added and reaction mixture was refluxed for 16 h. Reaction mixture was cooled to RT and concentrated *in vacuo*. The solid residue was dissolved in aqueous hydrochloric acid solution (0.3 M, 30 mL) and extracted with DCM (3 × 30 mL). The aqueous layer was then basified with aqueous sodium hydroxide solution (2 M) to pH 8 and subsequently extracted with EtOAc (2 × 30 mL). The DCM extracts were concentrated *in vacuo* and the resulting solid was carried out according to the abovementioned procedure three times more. All EtOAc extracts were combined, dried over $MgSO_4$, and concentrated *in vacuo* to afford **7** as white solid (206 mg).

Yield: 70 %

M. w.: 294.35

Exact mass: 294.14 calculated for $C_{18}H_{18}N_2O_2$

LRMS (ES^+) *m/z* (%): 295 (100) $[M + H]^+$

R_f: 0.45 (*n*-heptane:EtOAc 1:1)

M. p.: 124 – 125 °C (127 – 128 °C in reference [19])

^{1}H NMR (400 MHz, $CDCl_3$-*d*) δ 7.89 – 7.81 (m, 3H), 7.43 – 7.33 (m, 3H), 7.12 – 6.99 (m, 2H), 6.86 – 6.80 (m, 1H), 3.91 (t, *J* = 7.3 Hz, 2H), 3.84 (s, 3H), 2.50 (t, *J* = 7.4 Hz, 2H), 2.08 (p, *J* = 7.3 Hz, 2H).

^{13}C NMR (101 MHz, $CDCl_3$-*d*) δ 167.67, 159.40, 153.05, 141.52, 132.45, 130.76, 128.51, 123.10, 123.01, 122.47, 121.52, 120.40, 51.56, 50.61, 29.17, 19.75.

1-Phenyl-1,2,3,9-tetrahydro-4*H*-pyrrolo[2,3-*b*]quinolin-4-one (8)

Solution of amidine intermediate **7** (0.10 g, 0.33 mmol) in THF (25 mL) was cooled to -78 °C and stirred for 15 min. Lithium bis(trimethylsilyl)amide (1.0 mL, 1.0 M in THF/hexane) was added dropwise to the reaction mixture, warmed to 0 °C and stirred for 3 h. The reaction was quenched with saturated aqueous ammonium chloride solution (2 mL). Additional aqueous ammonium chloride solution (50 mL) was added. The aqueous phase was extracted with DCM (3 × 30 mL). Combined organic extracts were dried over $MgSO_4$ and concentrated to dryness. Purification by column chromatography on silica gel eluting with DCM:MeOH 20:1 (R_f = 0.34) afforded off-white solid (78 mg).

Yield: 91 %

M. w.: 262.31

Exact mass: 262.11 calculated for $C_{17}H_{14}N_2O$

LRMS (ES^+) *m/z* (%): 263 (100) $[M + H]^+$

R_f: 0.34 (DCM:MeOH 20:1)

M. p.: 181 – 182 °C (189 – 190 °C in reference [19])

^{1}H NMR (250 MHz, DMSO-d_6) δ 8.16 – 8.03 (m, 2H), 7.99 (d, *J* = 7.4 Hz, 1H), 7.61 (d, *J* = 8.0 Hz, 1H), 7.54 – 7.46 (m, 1H), 7.47 – 7.34 (m, 2H), 7.30 – 7.17 (m, 1H), 7.10 – 6.95 (m, 1H), 4.10 (t, *J* = 8.0 Hz, 2H), 3.19 (t, *J* = 7.9 Hz, 2H).

^{13}C NMR (63 MHz, DMSO-d_6) δ 143.43, 129.99, 129.91, 127.28, 123.42, 123.07, 122.72, 122.34, 118.82, 49.45, 23.32.

(3a*S*)-3a-hydroxy-1-phenyl-1,2,3,3a-tetrahydro-4*H*-pyrrolo[2,3-*b*]quinolin-4-one (9)

To the solution of quinolone intermediate **7** (0.015 g, 0.06 mmol) in THF (3 mL) cooled to -78 °C solution of lithium bis(trimethylsilyl)amide (69 μL, 1.0 M in THF) was added dropwise. The reaction mixture was stirred at -78 °C for 30 min. Subsequently solution of (-)-Davis reagent **19** (0.041 g, 0.14 mmol) in THF (3 mL) was added. The reaction mixture was stirred and slowly warmed to -10 °C over 16 h. The reaction was quenched with saturated aqueous ammonium chloride solution (5 mL) at -10 °C. MTBE (5 mL) was added and the reaction mixture was warmed to RT. Further, saturated aqueous sodium thiosulfate solution (5 mL) was added and reaction mixture was extracted with MTBE (2 × 15 mL). Collected organic layers were dried over $MgSO_4$ and concentrated to dryness. The resulting solid was partitioned between DCM (100 mL) and aqueous hydrochloric acid solution (0.3 M, 100 mL). The aqueous layer was washed with DCM (3 × 100 mL), basified with aqueous sodium hydroxide solution (2.0 M) to pH 8 and extracted with EtOAc (2 × 100 mL). Ethyl acetate organic extracts were dried over $MgSO_4$ and concentrated *in vacuo* to get desired final product **9** as bright yellow solid. Subsequently, compound **9** was recrystallized from acetonitrile (9 mg).

Yield: 57 %

M. w.: 278.31

Exact mass: 278.11 calculated for $C_{17}H_{14}N_2O_2$

LRMS (ES^+) *m/z* (%): 279 (100) $[M + H]^+$

R_f: 0.30 (DCM:MeOH 30:1)

M. p.: 191 – 192 °C (melting point was not determined in reference [19])

ee 70 % as determined by chiral HPLC analysis (*n*-hexane-ethanol 96.25 : 3.75, major enantiomer: t_R = 41.26 min, minor enantiomer: t_R = 47.99 min).

^{1}H NMR (300 MHz, $CDCl_3$-*d*:MeOH-d_4 10:1) δ 7.89 – 7.77 (m, 3H), 7.52 – 7.33 (m, 3H), 7.25 – 7.11 (m, 2H), 7.08 – 6.98 (m, 1H), 4.27 – 4.09 (m, 1H), 3.87 (t, *J* = 9.1 Hz, 1H), 2.53 – 2.35 (m, 1H), 2.33 – 2.13 (m, 1H).

^{13}C NMR (75 MHz, $CDCl_3$-*d*:MeOH-d_4 10:1) δ 195.21, 165.46, 151.48, 139.94, 136.36, 128.92, 127.19, 126.06, 124.81, 123.48, 120.92, 73.31, 29.64, 29.06.

4.3.2 SYNTHESIS OF 6-ETHYL ANALOGUE OF BLEBBISTATIN (SCHEME 4)

Methyl 2-amino-5-bromobenzoate (11)

To the solution of 5-bromoantranilic acid (**10**, 2.0 g, 9.26 mmol) in anhydrous MeOH (50 mL) cooled to 0 °C thionyl chloride (1.7 mL, 23.15 mmol) was added dropwise. The reaction mixture was refluxed for 24 h. The solvent was evaporated. Saturated aqueous sodium bicarbonate solution (100 mL) was added to crude residue and extracted with MTBE (3 × 100 mL). Combined organic layers were washed with brine, dried over Na_2SO_4 and concentrated to dryness. Purification by column chromatography on silica gel eluting with petroleum ether:EtOAc 2:1 (R_f = 0.85) gave the desired product **11** as yellowish solid (1.26 g).

Yield: 59 %

M. w.: 230.06

Exact mass: 228.97 calculated for $C_8H_8BrNO_2$

LRMS (ES^+) *m/z* (%): 231 (100) $[M + H]^+$

R_f: 0.85 (PE:EtOAc 2:1)

M. p.: 73 – 74 °C

^{1}H NMR (300 MHz, $CDCl_3$-*d*:MeOH-d_4 10:1) δ 7.89 – 7.77 (m, 3H), 7.52 – 7.33 (m, 3H), 7.25 – 7.11 (m, 2H), 7.08 – 6.98 (m, 1H), 4.27 – 4.09 (m, 1H), 3.87 (t, *J* = 9.1 Hz, 1H), 2.53 – 2.35 (m, 1H), 2.33 – 2.13 (m, 1H).

^{13}C NMR (75 MHz, $CDCl_3$-*d*:MeOH-d_4 10:1) δ 195.21, 165.46, 151.48, 139.94, 136.36, 128.92, 127.19, 126.06, 124.81, 123.48, 120.92, 73.31, 29.64, 29.06.

Methyl 5-bromo-2-[*(E)*-(1-phenylpyrrolidin-2-ylidene)amino]benzoate (12)

To the solution of *N*-phenyl-2-pyrrolidone (**2**, 0.35 g, 2.17 mmol) in DCM (3 mL) phosphoryl chloride (219 μL, 2.4 mmol) was added dropwise and stirred at RT for 3 h. Then solution of methyl 5-bromoanthranilate (**11**, 219 μL, 2.17 mmol) in DCM (12 mL) was added and the reaction mixture was refluxed for 16 h. Reaction mixture was cooled to RT and concentrated *in vacuo*. The solid residue was dissolved in aqueous hydrochloric acid solution (0.3 M, 100 mL) and extracted with DCM (3 × 100 mL). The aqueous layer was then basified with aqueous sodium hydroxide solution (2 M) to pH 8 and extracted with EtOAc (2 × 100 mL). The DCM extracts were concentrated *in vacuo* and the resulting solid was carried out according to the abovementioned procedure three times more. All EtOAc extracts were combined, dried over $MgSO_4$, and concentrated *in vacuo* to get the desired product **12** as off-white oil (180 mg).

Yield: 22 %

M. w.: 373.24

Exact mass: 372.05 calculated for $C_{18}H_{17}BrN_2O_2$

LRMS (ES^+) *m/z* (%): 374 (100) $[M + H]^+$

R_f: 0.24 (PE:EtOAc 4:1)

^{1}H NMR (300 MHz, $CDCl_3$-*d*) δ 7.98 (d, *J* = 2.4 Hz, 1H), 7.83 – 7.74 (m, 2H), 7.46 (dd, *J* = 8.5, 2.4 Hz, 1H), 7.41 – 7.32 (m, 2H), 7.13 – 7.04 (m, 1H), 6.71 (d, *J* = 8.5 Hz, 1H), 3.89 (t, *J* = 7.3 Hz, 2H), 3.84 (s, 3H), 2.47 (t, *J* = 7.4 Hz, 2H), 2.14 – 2.00 (m, 2H).

^{13}C NMR (75 MHz, $CDCl_3$-*d*) δ 166.26, 159.78, 152.35, 141.14, 135.45, 133.48, 133.44, 128.65, 125.17, 123.83, 123.39, 120.59, 113.92, 52.06, 50.81, 29.36, 19.74.

6-Bromo-1-phenyl-1,2,3,9-tetrahydro-4*H*-pyrrolo[2,3-*b*]quinolin-4-one (13)

Solution of amidine intermediate **12** (0.28 g, 0.75 mmol) in THF (25 mL) was cooled to -78 °C and stirred for 15 min. Lithium bis(trimethylsilyl)amide (2.25 mL, 1.0 M in THF/hexane) was added dropwise to the reaction mixture, warmed to 0 °C and stirred for 3 h. The reaction was quenched with saturated aqueous ammonium chloride solution (5 mL). Additional aqueous ammonium chloride solution (100 mL) was added. The aqueous phase was extracted with DCM (3 × 100 mL). Combined organic extracts were dried over $MgSO_4$ and concentrated to dryness. Purification by column chromatography on silica gel eluting with DCM:MeOH 20:1 (R_f = 0.26) afforded the desired product **13** as off-white solid (183 mg).

Yield: 72 %

M. w.: 341.20

Exact mass: 340.02 calculated for $C_{17}H_{13}BrN_2O$

LRMS (ES^+) *m/z* (%): 342 (100) $[M + H]^+$

R_f: 0.26 (DCM:MeOH 20:1)

M. p.: 154 –155 °C

^{1}H NMR (300 MHz, DMSO-d_6) δ 10.82 (bs, 1H), 8.14 – 7.94 (m, 3H), 7.62 – 7.47 (m, 2H), 7.43 – 7.31 (m, 2H), 7.08 – 6.95 (m, 1H), 4.07 (t, *J* = 7.9 Hz, 2H), 3.16 (t, *J* = 7.8 Hz, 2H).

^{13}C NMR (75 MHz, DMSO-d_6) δ 160.71, 153.42, 147.49, 142.26, 131.80, 129.03, 123.80, 121.73, 118.06, 114.37, 108.03, 105.81, 99.98, 48.74, 22.31.

6-Ethyl-1-phenyl-1,2,3,9-tetrahydro-9*H*-pyrrolo[2,3-*b*]quinolin-4-one (14)

To the solution of corresponding quinolinone intermediate **13** (0.08 g, 0.23 mmol) in DMA (10 mL) were successively added: stock solution of Ni(dppe)Cl_2 (5 mol%) and stock solution of neat diethylzinc (0.11 g, 0.92 mmol) in DMA (5 mL). The reaction mixture was stirred at 50 °C for 16 h. Subsequently, the reaction mixture was quenched with MeOH (5 mL) and thereafter saturated aqueous ammonium chloride solution (5 mL) was added. The mixture was extracted with MTBE (3 × 20 ml). Collected organic layers were washed with brine, dried over $MgSO_4$ and concentrated to dryness. Purification by column chromatography on silica gel using DCM:MeOH (30:1 → 20:1 → 10:1) as gradient eluent afforded desired product **14** as off-white solid (55 mg).

Yield: 70 %

M. w.: 290.36

Exact mass: 290.14 calculated for $C_{19}H_{18}N_2O$

LRMS (ES^+) *m/z* (%): 292 (100) $[M + H]^+$

R_f: 0.24 (DCM:MeOH 30:1)

M. p.: 120 – 121 °C

^{1}H NMR (300 MHz, DMSO-d_6) δ 8.02 (d, *J* = 7.3 Hz, 2H), 7.78 (d, *J* = 1.5 Hz, 1H), 7.52 (d, *J* = 8.4 Hz, 1H), 7.43 – 7.28 (m, 3H), 7.06 – 6.93 (m, 1H), 4.06 (t, *J* = 8.1 Hz, 2H), 3.15 (t, *J* = 8.1 Hz, 2H), 2.70 (q, *J* = 7.5 Hz, 2H), 1.23 (t, *J* = 7.6 Hz, 3H).

^{13}C NMR (75 MHz, DMSO-d_6) δ 142.55, 137.55, 129.64, 129.00, 1241.39, 119.91, 119.87, 118.06, 117.88, 106.50, 106.40, 48.79, 28.50, 22.45, 16.24.

(3a*S*)-6-Ethyl-3a-hydroxy-1-phenyl-1,2,3,3a-tetrahydro-4*H*-pyrrolo[2,3-*b*]quinolin-4-one (15)

To the solution of quinolone intermediate **14** (0.023 g, 0.08 mmol) in THF (4 mL) cooled to -78 °C solution of lithium bis(trimethylsilyl)amide (100 µL, 1.0 M in THF) was added dropwise. The reaction mixture was stirred at -78 °C for 30 min. Solution of (-)-Davis reagent 19 (0.061 g, 0.2 mmol) in THF (5 mL) was added. The reaction mixture was stirred and slowly warmed to -10 °C during 16 h. The reaction was quenched with saturated aqueous ammonium chloride solution (5 mL) at -10 °C. MTBE (5 mL) was added and the reaction mixture was warmed to RT. Further saturated aqueous sodium thiosulfate solution (5 mL) was added and reaction mixture was extracted with MTBE (2 × 15 mL). Collected organic layers were dried over MgSO4 and concentrated in vacuo. The resulting solid was partitioned between dichloromethane (100 mL) and aqueous hydrochloric acid solution (0.3 M, 100 mL). The aqueous phase was washed with dichloromethane (3 × 100 mL), basified with aqueous sodium hydroxide solution (2.0 M) to pH 8 and extracted with EtOAc (2 × 100 mL). The ethyl acetate organic extracts were dried over MgSO4 and concentrated to dryness to get the desired final product 15 as bright yellow solid. Subsequently, compound **15** was recrystallized from acetonitrile (12 mg).

Yield: 50 %

M. w.: 306.36

Exact mass: 306.14 calculated for $C_{19}H_{15}N_2O_2$

LRMS (ES^+) *m/z* (%): 307 (100) $[M + H]^+$

R_f: 0.24 (DCM:MeOH 30:1)

M. p.: 170 – 171 °C

ee 88 % as determined by chiral HPLC analysis (*n*-hexane-ethanol 96.25 : 3.75, major enantiomer: t_R = 31.45 min, minor enantiomer: t_R = 39.28 min).

^{1}H NMR (300 MHz, $CDCl_3$-*d*:MeOH-d_4 10:1) δ 7.81 (d, *J* = 7.8 Hz, 2H), 7.64 (d, *J* = 2.0 Hz, 1H), 7.44 – 7.33 (m, 2H), 7.32 – 7.28 (m, 1H), 7.20 – 7.08 (m, 2H), 4.20 – 4.06 (m, 1H), 3.85 (t, *J* = 9.0 Hz, 1H), 2.58 (q, *J* = 7.6 Hz, 2H), 2.48 – 2.35 (m, 1H), 2.31 – 2.14 (m, 1H), 1.19 (t, *J* = 7.6 Hz, 3H).

^{13}C NMR (75 MHz, $CDCl_3$-*d*:MeOH-d_4 10:1) δ 195.40, 165.09, 149.26, 140.02, 139.64, 136.22, 128.88, 125.94, 124.64, 120.79, 120.58, 73.27, 29.06, 28.02, 15.35.

(3a*R*)-6-ethyl-3a-hydroxy-1-phenyl-1,2,3,3a-tetrahydro-4*H*-pyrrolo[2,3-*b*]quinolin-4-one (16)

To the solution of quinolone intermediate **14** (0.023 g, 0.08 mmol) in THF (4 mL) cooled to -78 °C solution of lithium bis(trimethylsilyl)amide (100 µL, 1.0 M in THF) was added dropwise. The reaction mixture was stirred at -78 °C for 30 min. Solution of (+)-Davis reagent **20** (0.061 g, 0.2 mmol) in THF (0.04 mmol/1 mL) was added. The reaction mixture was stirred and slowly warmed to -10 °C over 16 h. The reaction was quenched with saturated aqueous ammonium chloride solution (5 mL) at -10 °C. MTBE (5 mL) was added and the reaction mixture was warmed to RT. Further saturated aqueous sodium thiosulfate solution (5 mL) was added and reaction mixture was extracted with MTBE (2 × 15 mL). Combined organic extracts were dried over $MgSO_4$ and concentrated *in vacuo.* The resulting solid was partitioned between dichloromethane (100 mL) and aqueous hydrochloric acid solution (0.3 M, 100 mL). The aqueous phase was washed with DCM (3 × 100 mL), basified with aqueous sodium hydroxide solution (2.0 M) to pH 8 and extracted with EtOAc (2 × 100 mL). Ethyl acetate organic layers were dried over $MgSO_4$ and concentrated *in vacuo* to obtain desired final product **16** as bright yellow solid. Subsequently, compound **16** was recrystallized from acetonitrile (12 mg).

Yield: 50 %

M. w.: 306.36

Exact mass: 306.14 calculated for $C_{19}H_{15}N_2O_2$

LRMS (ES^+) *m/z* (%): 307 (100) $[M + H]^+$

R_f: 0.24 (DCM:MeOH 30:1)

M. p.: 170 – 171 °C

ee 98 % as determined by chiral HPLC analysis (*n*-hexane-ethanol 96.25 : 3.75, major enantiomer: t_R = 39.28 min, minor enantiomer: t_R = 31.69 min).

^{1}H NMR (300 MHz, $CDCl_3$-*d*:MeOH-d_4 10:1) δ 7.82 (d, *J* = 7.9 Hz, 2H), 7.69 – 7.61 (m, 1H), 7.45 – 7.33 (m, 2H), 7.33 – 7.28 (m, 1H), 7.20 – 7.08 (m, 2H), 4.23 – 4.05 (m, 1H), 3.85 (t, *J* = 9.0 Hz, 1H), 2.59 (q, *J* = 7.6 Hz, 2H), 2.50 – 2.33 (m, 1H), 2.32 – 2.12 (m, 1H), 1.19 (t, *J* = 7.6 Hz, 3H).

^{13}C NMR (75 MHz, $CDCl_3$-*d*:MeOH-d_4 10:1) δ 195.42, 165.08, 149.29, 140.04, 139.65, 136.23, 128.88, 125.96, 124.62, 120.78, 120.58, 73.26, 29.06, 28.03, 15.36.

4.3.3 SYNTHESIS OF 6-BROMO ANALOGUE OF BLEBBISTATIN (SCHEME 5)

(3a*S*)-6-Bromo-3a-hydroxy-1-phenyl-1,2,3,3a-tetrahydro-4*H*-pyrrolo[2,3-*b*]quinolin-4-one (17)

To the solution of quinolone intermediate **13** (0.029 g, 0.085 mmol) in THF (4 mL) cooled to -78 °C solution of lithium bis(trimethylsilyl)amide (100 μL, 1.0 M in THF) was added dropwise. The reaction mixture was stirred at -78 °C for 30 min. Solution of (-)-Davis reagent **19** (0.061 g, 0.2 mmol) in THF (0.04 mmol/1 mL) was added. The reaction mixture was stirred and slowly warmed to -10 °C over 16 h. The reaction was quenched with saturated aqueous ammonium chloride solution (5 mL) at -10 °C. MTBE (5 mL) was added and the reaction mixture was warmed to RT. Further saturated aqueous sodium thiosulfate solution (5 mL) was added and reaction mixture was extracted with MTBE (2 × 15 mL). Combined organic extracts were dried over $MgSO_4$ and concentrated *in vacuo*. The resulting solid was partitioned between dichloromethane (100 mL) and aqueous hydrochloric acid solution (0.3 M, 100 mL). The aqueous phase was washed with DCM (3 × 100 mL), basified with aqueous sodium hydroxide solution (2.0 M) to pH 8 and extracted with EtOAc (2 × 100 mL). Ethyl acetate organic layers were dried over $MgSO_4$ and concentrated *in vacuo* to obtain the desired final product **17** as bright yellow solid. Subsequently, compound **17** was recrystallized from acetonitrile (19 mg).

Yield: 63 %

M. w.: 357.20

Exact mass: 356.02 calculated for $C_{17}H_{13}BrN_2O_2$

LRMS (ES^+) *m/z* (%): 358 (100) $[M + H]^+$

R_f: 0.47 (DCM:MeOH 30:1)

M. p.: 199 – 200 °C

ee 98 % as determined by chiral HPLC analysis (*n*-hexane-ethanol 85 : 15, major enantiomer: t_R = 14.20 min, minor enantiomer: t_R = 15.20 min).

^{1}H NMR (300 MHz, $CDCl_3$-*d*:MeOH-d_4 10:1) δ 7.89 (d, *J* = 2.3 Hz, 1H), 7.80 (d, *J* = 7.8 Hz, 2H), 7.51 (dd, *J* = 8.5, 2.4 Hz, 1H), 7.45 – 7.34 (m, 2H), 7.22 – 7.12 (m, 1H), 7.08 (d, *J* = 8.6 Hz, 1H), 4.23 – 4.07 (m, 1H), 3.87 (t, *J* = 9.1 Hz, 1H), 2.48 – 2.35 (m, 1H),

2.31 – 2.17 (m, 1H).

^{13}C NMR (75 MHz, $CDCl_3$-*d*:MeOH-d_4 10:1) δ 193.97, 165.53, 150.50, 139.66, 138.63, 129.55, 128.94, 127.76, 125.09, 122.26, 121.04, 115.98, 73.21, 48.59, 28.96.

(3a*R*)-6-bromo-3a-hydroxy-1-phenyl-1,2,3,3a-dihydro-4*H*-pyrrolo[2,3-*b*]quinolin-4-one (18)

To the solution of quinolone intermediate **13** (0.029 g, 0.085 mmol) in THF (4 mL) cooled to -78 °C solution of lithium bis(trimethylsilyl)amide (100 µL, 1.0 M in THF) was added dropwise. The reaction mixture was stirred at -78 °C for 30 min. The solution of (+)-Davis reagent **20** (0.061 g, 0.2 mmol) in THF (0.04 mmol/1 mL) was added. The reaction mixture was stirred and slowly warmed to -10 °C over 16 h. The reaction was quenched with saturated aqueous ammonium chloride solution (5 mL) at -10 °C. MTBE (5 mL) was added and the reaction mixture was warmed to RT. Further saturated aqueous sodium thiosulfate solution (5 mL) was added and reaction mixture was extracted with MTBE (2 × 15 mL). Combined organic layers were dried over $MgSO_4$ and concentrated to dryness. The resulting solid was partitioned between dichloromethane (100 mL) and aqueous hydrochloric acid solution (0.3 M, 100 mL). The aqueous phase was washed with DCM (3 × 100 mL), basified with aqueous sodium hydroxide solution (2.0 M) to pH 8 and extracted with EtOAc (2 × 100 mL). Ethyl acetate organic layers were dried over $MgSO_4$ and concentrated *in vacuo* to obtain the desired final product **18** as bright yellow solid. Then compound **18** was recrystallized from acetonitrile (19 mg).

Yield: 63 %

M. w.: 357.20

Exact mass: 356.02 calculated for $C_{17}H_{13}BrN_2O_2$

LRMS (ES^+) *m/z* (%): 358 (100) $[M + H]^+$

R_f: 0.47 (DCM:MeOH 30:1)

M. p.: 199 – 200 °C

ee 98 % as determined by chiral HPLC analysis (*n*-hexane-ethanol 85 : 15, major enantiomer: t_R = 15.18 min, minor enantiomer: t_R = 14.15 min).

^{1}H NMR (300 MHz, $CDCl_3$-*d*:MeOH-d_4 10:1) δ 7.89 (d, *J* = 2.2 Hz, 1H), 7.80 (d, *J* = 7.9 Hz, 2H), 7.51 (dd, *J* = 8.5, 2.3 Hz, 1H), 7.45 – 7.33 (m, 2H), 7.22 – 7.13 (m, 1H), 7.08 (d, *J* = 8.5 Hz, 1H), 4.24 – 4.09 (m, 1H), 3.87 (t, *J* = 9.1 Hz, 1H), 2.51 – 2.33 (m, 1H), 2.33 – 2.17 (m, 1H).

^{13}C NMR (75 MHz, $CDCl_3$-*d*:MeOH-d_4 10:1) δ 193.98, 165.52, 150.51, 139.67, 138.63, 129.55, 128.95, 127.77, 125.09, 122.24, 121.05, 115.98, 48.59, 28.96.

4.4 RESULTS AND DISCUSSION

Present study was focused on synthesis of novel blebbistatin derivatives and searching for different or modified synthetic procedures providing easier synthesis of **5** and its analogues.

An interesting intermediate **13** has been synthetized from its precursor **12**. Intermediate **13** constitutes a facile access to several other blebbistatin derivatives via bromine substitution. The assumption about the reactivity of bromine at C6 position was confirmed by successful conversion of compound **13** to compound **14** using Negishi coupling procedure. All these compounds are novel and have not been reported in literature so far.

Synthesis of novel derivatives included at least one additional step – conversion of bromo-quinolinone intermediate **13** to another substituted quinolinone compound (, Scheme 6). Several cross coupling methods have been applied for preparation of ethyl derivative – primarily unsuccessful Suzuki-Miyaura[31] coupling, finally fruitful Negishi type coupling using Ni catalyst[29,30]. Sonogashira type coupling has been applied in an attempt to synthesize ethynyl compound **21**, unfortunately with negative results. However, further optimization of this cross coupling type reaction might bring the desired outcome.[32,33]

As a result, five final products **9**, **15**, **16**, **17**, **18** were prepared as potential uncompetitive myosin inhibitors. Compound **9** have previously been reported by Lucas-Lopez ae co-workers [17], the remaining products are new compounds. However, only the results of subsequent biological assays will help to characterize the properties of these compounds as well as relationship between the blebbistatin, its derivatives and myosin more specifically.

Additionally, an alternative synthetic route to amidine synthesis (Scheme 2) was investigated with unsatisfactory results. However, this study left a hint, which can be utilized in further investigation of this reaction.

5 CONCLUSION

The aim of this work was to prepare novel blebbistatin derivatives as potential small molecule myosin inhibitors. As myosin proteins are involved in several cell processes their dysfunctions and mutations can lead to a progression of diseases or genetic syndromes. Therefore, development of novel myosin inhibitors has a great potential in order to understand myosin cellular functions as well as to improve current treatment of diseases associated with myosins.

6 REFERENCES

1. HARTMAN, M. A., SPUDICH, J. A. The myosin superfamily at a glance. *J. Cell Sci.* [online]. 2012, Vol. 125, p. 1627–1632. DOI 10.1242/jcs.094300.
   Available from: http://www.ncbi.nlm.nih.gov/pmc/articles/PMC3346823/. (accessed May 2, 2016).

2. BOND, L. M, TUMBARELLO, D. A., KENDRICK-JONES, J., BUSS, F. Small-molecule inhibitors of myosin proteins. *Future Med. Chem.* [online]. 2013, Vol. 5, no. 1, p. 41–52. DOI 10.4155/fmc.12.185.
   Available from: http://www.ncbi.nlm.nih.gov/pmc/articles/PMC3971371/. (accessed May 2, 2016).

3. SYAMALADEVI, D. P., SPUDICH, J. A., SOWDHAMINI, R. Structural and functional insights on the myosin superfamily. *Bioinform. Biol. Insights* [online]. 2012, Vol. 6, p. 11–21. DOI 10.4137/BBI.S8451.
   Available from: http://www.ncbi.nlm.nih.gov/pmc/articles/PMC3290112/.(accessed May 2, 2016).

4. Myosin: The Actin Motor Protein. In: LODISH, H., BERK, A., ZIPURSKY, S. L., MATSUDAIRA, P., BALTIMORE, D., DARNELL, J. eds. *Molecular Cell Biology.* 4th ed. [online]. New York: W. H. Freeman, 2000. ISBN-10: 0-7167-3136-32000.
   Available from: http://www.ncbi.nlm.nih.gov/books/NBK21475/.(accessed May 2, 2016).

5. VICENTE-MANZANARES, M., MA, X., ADELSTEIN, R. S., HORWITZ, A. R. Non-muscle myosin II takes centre stage in cell adhesion and migration. *Nat. Rev. Mol. Cell Biol.* [online]. 2009, Vol. 10, no. 11, p. 778–790. DOI 10.1038/nrm2786.
   Available from: http://www.nature.com/nrm/journal/v10/n11/abs/nrm2786.html. (accessed May 2, 2016).

6. CHENEY, R. E., MOOSEKER, M. S. Unconventional myosins. *Curr. Opin. Cell Biol*. [online]. 1992, Vol. 4, no. 1, p. 27–35. DOI 10.1016/0955-0674(92)90055-H.
   Available from: http://www.sciencedirect.com/science/article/pii/095506749290055H. (accessed May 2, 2016).

7. KENDRICK-JONES, J., HODGE, T. P., LISTER, I. M. B., ROBERTS, R. C., BUSS, F. Myosin superfamily [online].
   Available from: http://www.mrc-lmb.cam.ac.uk/myosin/Review/Reviewframeset.html. (accessed May 2, 2016).

8. SELLERS, J. R. Myosins: A diverse superfamily. *Biochim. Biophys. Acta, Mol. Cell Res*. [online]. 2000, Vol. 1496, no. 1, p. 3–22. DOI 10.1016/S0167-4889(00)00005-7. Available from: http://www.sciencedirect.com/science/article/pii/S0167488900000057. (accessed May 2, 2016).

9. SPARKES, I. A. Motoring around the plant cell: insights from plant myosins. *Biochem. Soc. Trans.* [online]. 2010, Vol. 38, no. 3, p. 833–838. DOI 10.1042/BST0380833. Available from: http://www.biochemsoctrans.org/content/38/3/833.full-text.pdf. (accessed May 2, 2016).

10. HODGE, T., COPE, M. J. T. V. A Myosin Family Tree. *J. Cell Sci*. [online]. 2000, Vol. 113, no. 19, p. 3353–3354. Available from: http://jcs.biologists.org/content/joces/113/19/3353.full.pdf. (accessed May 2, 2016).

11. MBInfo contributors. The myosin superfamily of motor proteins. In: *MBInfo Wiki*. Available from: http://www.mechanobio.info/figure/figure/1391394893116.jpg.html. (accessed May 2, 2016).

12. MBInfo contributors. The "power stroke" mechanism for myosin movement along actin filaments. In: *MBInfo Wiki*. Available from: http://www.mechanobio.info/figure/figure/1384245241982.jpg.html. (accessed May 2, 2016).

13. CLARK, K., LANGESLAG, M., FIGDOR, C. G., VAN LEEUWEN, F. N. Myosin II and mechanotransduction: a balancing act. *Trends Cell Biol*. [online]. 2007, Vol. 17, no. 4, p. 178–186. DOI 10.1016/j.tcb.2007.02.002. Available from: https://www.researchgate.net/publication/6486691_Myosin_II_and_mechanotransduction_a_balancing_act_Trends_Cell_Biol_17_178-186. (accessed May 2, 2016).

14. OUDERKIRK, J. L.; KRENDEL, M. Non-muscle myosins in tumor progression, cancer cell invasion, and metastasis. *Cytoskeleton* [online] 2014, Vol. 71, no. 8, p. 447–463. DOI 10.1002/cm.21187. Available from: http://onlinelibrary.wiley.com/doi/10.1002/cm.21187/epdf. (accessed May 2, 2016).

15. KOVÁCS, M., TÓTH, J., HETÉNYI, C., MÁLNÁSI-CSIZMADIA, A., SELLER, J. R. Mechanism of blebbistatin inhibition of myosin II. *J. Biol. Chem.* [online]. 2004, Vol. 279, no. 34, p. 35557–35563. DOI 10.1074/jbc.M405319200. Available from: http://www.jbc.org/content/279/34/35557.full.pdf. (accessed May 2, 2016).

16. STRAIGHT, A. F., CHEUNG, A., LIMOUZE, J., CHEN, I., WESTWOOD, N. J, SELLERS, J. R., MITCHISON, T. J. Dissecting temporal and spatial control of cytokinesis with a myosin II inhibitor. *Science* [online]. 2003, Vol. 299, no. 5613, p. 1743–1747. DOI 10.1126/science.1081412.
Available from: http://science.sciencemag.org/content/299/5613/1743.full. (accessed May 2, 2016).

17. LUCAS-LOPEZ, C., PATTERSON, S., BLUM, T., STRAIGHT, A. F., TOTH, J., SLAWIN, A. M. Z., MITCHISON, T. J., SELLERS, J. R., WESTWOOD, N. J. Absolute stereochemical assignment and fluorescence tuning of the small molecule tool, (-)-blebbistatin. *Eur. J. Org. Chem.* [online]. 2005, No. 9, p. 1736–1740. DOI 10.1002/ejoc.200500103.
Available from: http://onlinelibrary.wiley.com/enhanced/doi/10.1002/ejoc.200500103. (accessed May 2, 2016).

18. PATTERSON, S., LUCAS-LOPEZ, C., WESTWOOD, N. J. Selective chemical intervention in biological systems: the small molecule tool (*S*)-(-)-Blebbistatin. In: HICKS, M. G., KETTNER, C. eds. *Proceedings of the International Beilstein Workshop: The Chemical Theatre of Biological Systems*, May 24th – 28th, 2004, Bozen Italy [online]. Frankfurt: Beilstein Institut, 2005, p. 147–166. ISBN 3-8325-1019-2.
Available from: www.beilstein-institut.de/download/698/buch.pdf. (accessed May 2, 2016).

19. LUCAS-LOPEZ, C., ALLINGHAM, J. S, LEBL, T., LAWSON, C. P. A. T, BRENK, R., SELLERS, J. R, RAYMENT, I., WESTWOOD, N. J. The small molecule tool (*S*)-(-)-blebbistatin: novel insights of relevance to myosin inhibitor design. *Org. Biomol. Chem.* [online]. 2008. Vol. 6, no. 12, p. 2076–2084. DOI 10.1039/b801223g.
Available from: http://www.ncbi.nlm.nih.gov/pmc/articles/PMC3758137/. (accessed May 2, 2016).

20. ALLINGHAM, J. S., SMITH, R., RAYMENT, I. The structural basis of blebbistatin inhibition and specificity for myosin II. *Nat. Struct. Mol. Biol.* [online]. 2005, Vol. 12, no. 4, p. 378–379. DOI 10.1038/nsmb908.
Available from: http://www.nature.com/nsmb/journal/v12/n4/pdf/nsmb908.pdf. (accessed May 2, 2016).

21. TÓTH, J. *Functional characterization of a novel myosin and a novel myosin inhibitor*. PhD Thesis [online]. Biology Doctoral School at ELTE TTK, Budapest, 2006.
Available from: http://www.mk-lab.org/downloads/dolgozatok/Toth_PhD.pdf. (accessed May 2, 2016).

22. MIKULICH, A., KAVALIAUSKIENE, S. JUZENAS, P. Blebbistatin, a myosin inhibitor, is phototoxic to human cancer cells under exposure to blue light. *Biochim. Biophys. Acta, Gen. Subj*. [online]. 2012, Vol. 1820, no. 7, p. 870–877. DOI 10.1016/j.bbagen.2012.04.003.
Available from: http://www.sciencedirect.com/science/article/pii/S0304416512000967. (accessed May 2, 2016).

23. KÉPIRÓ, M., VÁRKUTI, B. H., VÉGNER, L., VÖRÖS, G., HEGYI, G., VARGA, M., MÁLNÁSI-CSIZMADIA, A. *para*-Nitroblebbistatin, the non-cytotoxic and photostable myosin II inhibitor. *Angew. Chem., Int. Ed.* [online]. 2014, Vol. 53, no. 31, p. 8211–8215. DOI 10.1002/anie.201403540.
Available from: http://onlinelibrary.wiley.com/doi/10.1002/anie.201403540/pdf. (accessed May 2, 2016).

24. KÉPIRÓ, M., VÁRKUTI, B. H., BODOR, A., HEGYI, G., DRAHOS, L., KOVÁCS, M., MÁLNÁSI-CSIZMADIA, A. Azidoblebbistatin, a photoreactive myosin inhibitor. *Proc. Natl. Acad. Sci. U. S. A.* [online]. 2012, Vol. 109, no. 24, p. 9402–9407. DOI 10.1073/pnas.1202786109.
Available from: http://www.pnas.org/content/109/24/9402.full.pdf. (accessed May 2, 2016).

25. CHARETTE, A. B., GRENON, M. Mild method for the synthesis of amidines by the electrophilic activation of amides. *Tetrahedron Lett.* [online]. 2000, Vol. 41, no. 11, p. 1677–1680. DOI 10.1016/S0040-4039(00)00040-X.
Available from: http://www.sciencedirect.com/science/article/pii/S004040390000040X. (accessed May 2, 2016).

26. SFORZA, S., DOSSENA, A., CORRADINI, R., VIRGILI, E., MARCHELLI, R. Tf20/amide adducts: versatile reagents for the synthesis of imidates and amidines. *Tetrahedron Lett*. [online]. 1998, Vol. 39, no. 2, p. 711–714. DOI 10.1016/S0040-4039(97)10642-10646.
Available from: http://www.sciencedirect.com/science/article/pii/S0040403997106426. (accessed May 2, 2016).

27. BERMAN, H. M., WESTBROOK, J., FENG, Z., GILLILAND, G., BHAT, T. N, WEISSIG, H., SHINDYALOV, I. N., BOURNE, P. E. The Protein Data Bank. *Nucleic Acids Res*. [online]. 2000, Vol. 28, no. 1, p. 235–242. DOI 10.1093/nar/28.1.235.
Available from: http://nar.oxfordjournals.org/content/28/1/235.full.pdf+html. (accessed May 2, 2016).

28. WAGNER, K. *Synthese von Blebbistatin.* Bachelor Thesis, Friedrich-Schiller-Universität Jena, Faculty of Chemistry and Earth Science, Institute for Organic Chemistry and Macromolecular Chemistry, 2015.

29. HUO, S. Highly efficient, general procedure for the preparation of alkylzinc reagents from unactivated alkyl bromides and chlorides. *Org. Lett*. [online]. 2003, Vol. 5, no. 4, p. 423–425. DOI 10.1021/ol0272693.
Available from: http://pubs.acs.org/doi/pdf/10.1021/ol0272693. (accessed May 2, 2016).

30. HERBERT, J. M. Negishi-type coupling of bromoarenes with dimethylzinc. *Tetrahedron Lett*. [online]. 2004, Vol. 45, no. 4, p. 817–819. DOI 10.1016/j.tetlet.2003.11.018.
Available from: http://www.sciencedirect.com/science/article/pii/S004040390302728X. (accessed May 2, 2016).

31. LI, H., ZHONG, Y.-L., CHEN, C.-Y., FERRARO, A. E., WANG, D. A concise and atom-economical Suzuki-Miyaura coupling reaction using unactivated trialkyl- and triarylboranes with aryl halides. *Org. Lett*. [online]. 2015, Vol. 17, no. 14, p. 3616–3619. DOI 10.1021/acs.orglett.5b01720.
Available from: http://pubs.acs.org/doi/pdf/10.1021/acs.orglett.5b01720. (accessed May 2, 2016).

32. SUN, F., GU, Z. Decarboxylative alkynyl termination of palladium-catalyzed Catellani reaction: a facile synthesis of α-alkynyl anilines via *ortho* C-H amination and alkynylation. *Org. Lett*. [online]. 2015, Vol. 17, no. 9, p. 2222–2225. DOI 10.1021/acs.orglett.5b00830.
Available from: http://pubs.acs.org/doi/pdf/10.1021/acs.orglett.5b00830. (accessed May 2, 2016).

33. KOELLHOFER, A., PLENIO, H. A convenient high activity catalyst for the Sonogashira coupling of aryl bromides. *Adv. Synth. Catal.* [online] 2005. Vol. 347, no. 9, p. 1295–1300. DOI 10.1002/adsc.200505095.
Available from: http://onlinelibrary.wiley.com/doi/10.1002/adsc.200505095/pdf. (accessed May 2, 2016).